(12) mic

SMALL SCALE DISCHARGE STUDIES

M. Rokni, J.H. Jacob and J.A. Mangano
Avco Everett Research Laboratory, Inc.
2385 Revere Beach Parkway
Everett MA 02149

Semi–Annual Report for Period 1 September 1976 to 28 February 1977

Sponsored by
DEFENSE ADVANCED RESEARCH PROJECTS AGENCY
DARPA Order No. 1806

Monitored by
OFFICE OF NAVAL RESEARCH
DEPARTMENT OF THE NAVY
Arlington VA 22217

FOREWORD

DARPA Order No.: 1806

Program Code No.: 5E20

Name of Contractor: Avco Everett Research Laboratory, Inc.

Effective Date of Contract: 15 August 1974

Contract Expiration Date: 15 November 1977

Amount of Contract: $960,451

Contract No.: N00014-75-C-0062

Principal Investigator and Phone No.: J.H. Jacob
(617) 389-3000, Ext. 329

Scientific Officer: Director, Physics Program, Physical Sciences Div.
Office of Naval Research
Department of the Navy
800 North Quincy Street
Arlington, VA 22217

Short Title of Work: Laser Discharge Studies

UNCLASSIFIED

SECURITY CLASSIFICATION OF THIS PAGE (When Data Entered)

REPORT DOCUMENTATION PAGE	READ INSTRUCTIONS BEFORE COMPLETING FORM
1. REPORT NUMBER	2. GOVT ACCESSION NO. 3. RECIPIENT'S CATALOG NUMBER
4. TITLE (and Subtitle) (6) Small Scale Discharge Studies,	(9) 5. TYPE OF REPORT & PERIOD COVERED Semi-Annual Report, 1 Sept 1976 - 28 Feb 1977
	6. PERFORMING ORG. REPORT NUMBER
7. AUTHOR(s) (10) M. Rokni, J. H. Jacob and J. A. Mangano	(15) 8. CONTRACT OR GRANT NUMBER(s) N00014-75-C-0062, DARPA Order-1806
9. PERFORMING ORGANIZATION NAME AND ADDRESS Avco Everett Research Laboratory, Inc. 2385 Revere Beach Parkway Everett, MA 02149	10. PROGRAM ELEMENT, PROJECT, TASK AREA & WORK UNIT NUMBERS
11. CONTROLLING OFFICE NAME AND ADDRESS Defense Advanced Research Projects Agency DARPA Order No. 1806	12. REPORT DATE (11) 28 Feb 77 13. NUMBER OF PAGES 68
14. MONITORING AGENCY NAME & ADDRESS (if different from Controlling Office) Office of Naval Research Department of the Navy Arlington, VA 22217 (12) 68p.	15. SECURITY CLASS. (of this report) Unclassified 15a. DECLASSIFICATION/DOWNGRADING SCHEDULE
16. DISTRIBUTION STATEMENT (of this Report) Approved for Public Release; Distribution Unlimited.	
17. DISTRIBUTION STATEMENT (of the abstract entered in Block 20, if different from Report)	
18. SUPPLEMENTARY NOTES	
19. KEY WORDS (Continue on reverse side if necessary and identify by block number) Visible/UV Lasers Rare Gas Fluoride Lasers Rare Gas Fluoride Kinetics KrF* and ArF* Lasers	
20. ABSTRACT (Continue on reverse side if necessary and identify by block number) The dominant formation and quenching processes in e-beam pumped ArF* and KrF* lasers are discussed. The exciplexes are produced by irradiating Ar/F_2 and $Ar/Kr/F_2$ mixtures with a 5 A/cm^2, 150 keV e-beam. A steady state analysis is valid since the reaction times are short compared to the 300 nsec beam pulse length. The quenching of ArF* by F_2 and Ar has been measured by analyzing the ArF* ($B^2\Sigma_{1/2} \rightarrow X^2\Sigma_{1/2}$) fluorescence as a function of the F_2 and Ar partial pressures. We have also measured the displacement of the Ar in ArF* by Kr to form KrF*. The dominant quenching processes of →	

DD FORM 1 JAN 73 1473 EDITION OF 1 NOV 65 IS OBSOLETE

UNCLASSIFIED

SECURITY CLASSIFICATION OF THIS PAGE (When Data Entered)

Ø18750

B

(20)

KrF* were identified and the rate constants were measured. The ArF* and KrF* are formed from the ionic states with high efficiency. Interception of the precursers can be made negligible by choosing the experimental conditions properly. The quenching of KrF* by Ar and Kr is mainly a three body process resulting in the formation of Kr_2F^*. The emission from Kr_2F^* was observed in a broad band centered at 410 nm. We have verified that the Kr_2F^* is produced subsequent to the KrF* formation by performing a laser saturation experiment.

REPORT SUMMARY

This report describes in detail the formation and quenching kinetics in e-beam pumped ArF^* and KrF^* lasers. For moderate fast electron current densities and mixtures containing a few tenths of a percent F_2 the formation proceeds via the ionic channel. From our measurements we have determined that both the atomic and molecular rare gas ions recombine with F^- to form the rare gas fluoride exciplex. The quenching rate constants of ArF^* and KrF^* by Ar, Kr and F_2 have also been measured.

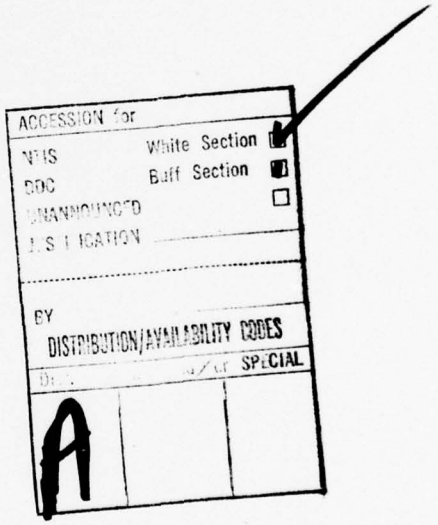

TABLE OF CONTENTS

LIST OF ILLUSTRATIONS

I. FORMATION AND QUENCHING PROCESSES IN E-BEAM PUMPED ArF* AND KrF* LASERS

1. INTRODUCTION

Much research has been performed on the rare gas monohalide exciplexes since their spectra was first reported by Velazco and Setser.[1] In the two years following the Velazco-Setser publication many of these molecules have been made to lase by both pure e-beam[2] and discharge pumping.[3] The most promising candidates that are scalable to high output power and efficiency are the rare gas fluorides.[4, 5] To facilitate the scaling of these lasers to high average power a detailed knowledge of the kinetic processes are necessary. Velazco, Kolts and Setser[6] have shown

(1) J.E. Velazco and D.W. Setser, "Quenching of the Xe Metastable Atoms," JQE 11, 708-709 (1975).

(2) J.J. Ewing and C.A. Brau, "Laser Action on the $^2\Sigma^+_{1/2} \rightarrow {}^2\Sigma^+_{1/2}$ Bands of KrF and XeCl," Appl. Phys. Lett. 27, 350-352 (1975).
C.A. Brau and J.J. Ewing, "354 nm Laser on XeF," Appl. Phys. Lett. 27, 435-437 (1975).
S.K. Searles and G.A. Hart, "Stimulated Emission at 281.8 nm from XeBr," Appl. Phys. Lett. 27, 243-245 (1975).
E.R. Ault, R.S. Bradford and M.L. Bhaumik, "High Power Xenon Fluoride Laser," Appl. Phys. Lett. 27, 413-415 (1975).

(3) J.A. Mangano and J.H. Jacob, "Electron Beam Controlled Discharge Pumping of KrF Laser," Appl. Phys. Lett. 27, 495-497 (1975).
R. Burnham, H.W. Harris and N. Djeu, "Xenon Fluoride Laser Excitation by Transverse Electric Discharge," Appl. Phys. Lett. 28, 86-87 (1976).
C.P. Wang, H. Mirels, D.G. Sutton and S.N. Suchard, "Fast Discharge Initiated XeF Laser," Appl. Phys. Lett. 28, 326-328 (1976).
J.A. Mangano, J.H. Jacob and J.B. Dodge, "Electron-Beam-Controlled Discharge Pumping of the XeF Laser," Appl. Phys. Lett. 29, 426-428 (1976).

(4) J.A. Mangano, et al, "An 8.5 Liter E-Beam Pumped KrF* Laser," (unpublished).

(5) R. Hunter (unpublished).

(6) J.E. Velazco, J.H. Kolts and D.W. Setser, "Quenching Rate Constants for Metastable Argon, Krypton, and Xenon Atoms by Fluorine Containing Molecules and Branching Ratios of XeF* and KrF* Formation," J. Chem. Phys. 65, 3468-3485 (1976).

that the rare gas fluorides are formed with high efficiency from excited rare gases. We will show that the rare gas ions also produce these exciplex species with high efficiency. The formation rate of these excited molecules is rapid since they can be accessed through an ion-channel: e-beam ionization of the rare gas followed by rapid dissociative electron attachment to the halogen and subsequent extremely rapid ion-ion recombination.

In this paper we will discuss the formation and quenching of the ArF* and KrF* exciplexes. The kinetic processes were investigated by irradiating mixtures of rare gases and fluorine by a beam of fast electrons. The fluorescence emanating from these mixes was monitored and recorded. The kinetic processes were isolated by studying the dependence of the fluorescence on the partial pressure of one of the constituents of the gas mixture, while the partial pressures of the remaining gases in the mixture were kept constant. By analyzing the dependence of the quasi-steady state fluorescence on the partial pressure of the rare gases and fluorine and the power deposited into the gas mixture, we obtained the various quenching rate constants. It should be noted that only relative intensity measurements were required by the analysis.(7)

In Section 2 the experimental apparatus used to make the measurements is presented. The formation and quenching processes in ArF* are presented and discussed in Section 3. A similar presentation for KrF* is made in Section 4.

2. EXPERIMENTAL SET-UP

The experimental set-up is shown schematically in Figure 1. The gas mixtures were excited by a high energy e-beam. The electrons were

(7) M. Rokni, J.H. Jacob, J.A. Mangano and R. Brochu, "Two and Three Body Quenching of XeF* by Ar and Xe," Appl. Phys. Lett. 30, 458-460 (1977).

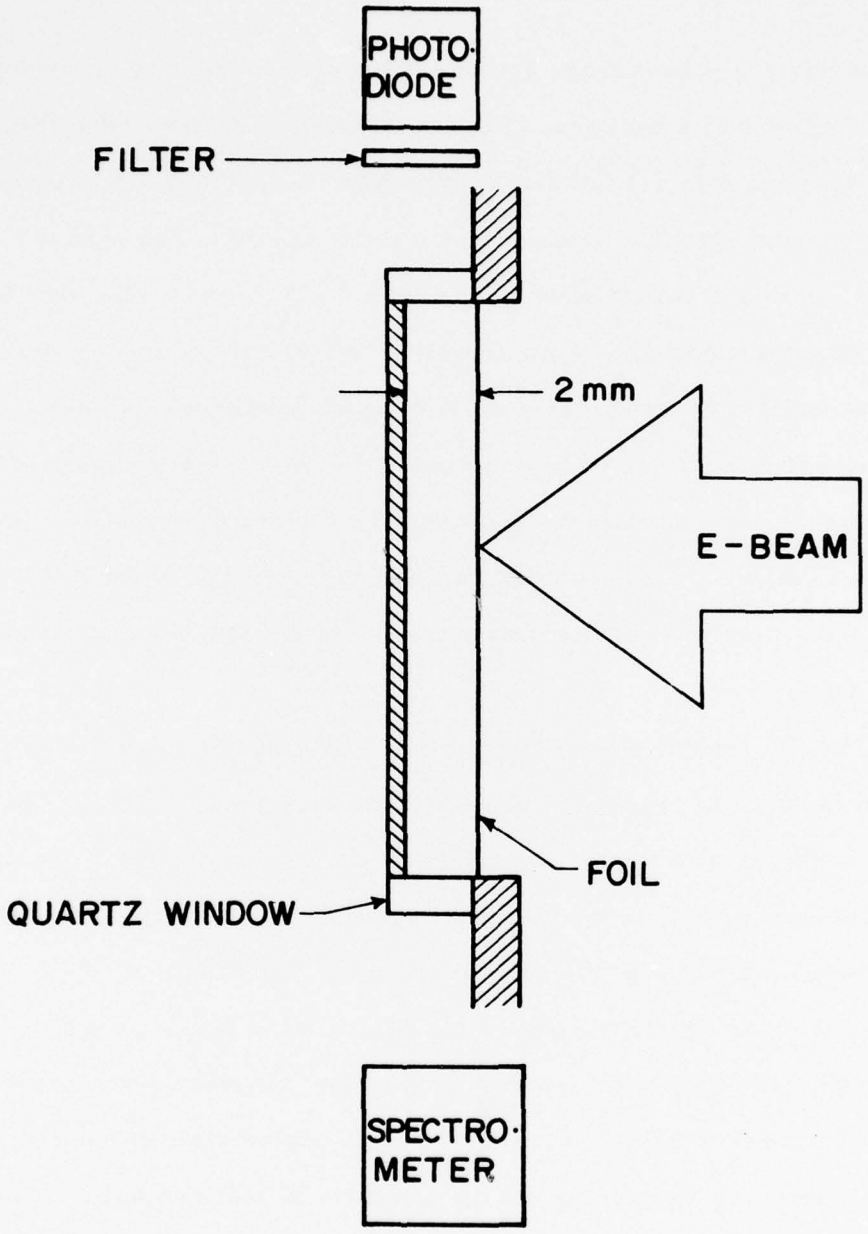

Figure 1 Schematic of Experimental Set-Up

generated from a cold cathode and accelerated to an energy of 150 keV in a vacuum chamber at a background pressure of $\leq 10^{-5}$ torr. The fast electrons passed through a 2 mil Kapton foil that separated the gas mixture from the high vacuum chamber containing the cold cathode. The mixture was contained in a teflon cell with dimensions $22 \times 2 \times 0.2$ cm^3. The dimension of the cell along the initial e-beam direction was 0.2 cm to ensure uniform energy deposition by the e-beam up to mixture pressures of 4 atm. The e-beam current density, after attenuation by the foil and supporting structure, was 5 A/cm^2. The current density could be further attenuated by introducing a partially transmitting screen on the high vacuum side of the foil. The e-beam pulse length was 300 nsec long, enabling the fluorescence amplitude to reach a steady state.

The fluorescence intensities were monitored by appropriate filters and photodiodes, and spectra were recorded on a 1 meter Hilger spectrograph. In the case of the ArF* radiation, the side of the filter facing the photodiode was coated with sodium salicylate. The sodium salicylate converts the 193 nm photons into visible and near UV radiation. Care was taken to ensure that the spectral width of the filters were large enough so that the transmitted radiation was representative of the overall kinetic processes.

The gases were premixed in a Teflon coated stainless steel tank. Adequate time was allowed to ensure complete diffusive mixing. The gas mixtures were introduced into the Teflon cell which could be evacuated to pressures of $\leq 10^{-4}$ torr. Research grade (Matheson) Ar and Xe were used without any further purification. The gases were analyzed by Gollob Analytical Service, Inc., and found to have less than 100 ppm of O_2, N_2, H_2O and CO_2 impurities. The F_2 was 98% pure.

3. FORMATION AND QUENCHING OF ArF*

Since Ar is the main constituent in most rare gas fluoride laser mixes, most of the e-beam energy is deposited in the argon. So it is reasonable to first investigate the kinetic processes in e-beam pumped Ar/F_2 mixes.

(a) Formation of ArF*

Table 1 lists the dominant formation kinetics for low current density (≤ 10 A/cm^2) e-beam pumped systems. About 55% of the e-beam energy deposited in the gas is channeled into Ar^+ formation as given by reaction (1). Approximately 10% of the deposited energy is channeled into Ar* formation by the energetic secondary electrons formed in reaction (1).[8]

For our experimental conditions, i.e., Ar pressures below 4 atm, mixtures containing ≥ 2 torr of F_2 and e-beam currents ≤ 5 A/cm^2, the main loss mechanism for secondary electrons is dissociative attachment by F_2 resulting in the formation of F^-. Hence the dominant ArF* formation mechanism proceeds via the ion channel (see reactions (4) and (7) in Table 1). If the pump power or pressure stated above are exceeded, dissociative recombination of e_s with Ar_2^+ ($e_s + Ar_2^+ \rightarrow Ar^* + Ar$) becomes important. The exciplex formation will then proceed via the metastable channel (reaction 5, Table 1). When the exciplex formation proceeds via the metastables, losses due to Penning ionization ($Ar^* + Ar^* \rightarrow Ar^+ + e_s + Ar$) and rare gas excimer formation (Ar_2^*) must be considered. Figure 2 shows the variation of e_s, F^-, Ar^+ and Ar_2^+ for a mixture containing 2 torr of F_2 plus Ar. The Ar_2^+ and

(8) L.R. Peterson and J.E. Allen, Jr., "Electron Impact Cross Sections for Argon," J. Chem. Phys. 56, 6068-6076 (1972).

TABLE 1. DOMINANT FORMATION KINETICS FOR ArF*

$\vec{e} + Ar$	→	$Ar^+ + \vec{e} + e_s$		(1)
$e_s + F_2$	→	$F^- + F$	5×10^{-9} cm^3/sec[18]	(2)
$e_s + Ar$	→	$Ar^* + e_s$		(3)
$F^- + Ar^+ + (M)$	→	$ArF^* + (M)$	$10^{-7} + 10^{-7}$ p;p < 1 atm	(4)
$Ar^* + F_2$	→	$ArF^* + F$		(5)

Pressure > 1 atm

$Ar^+ F^- + (M)$	→	$ArF^* + (M)$	1.1×10^{-6} cm^3/sec	(4a)
$Ar^+ + 2Ar$	→	$Ar_2^+ + Ar$	2.5×10^{-31} cm^6/sec[19]	(6)
$Ar_2^+ + F^-$	→	$ArF^* + Ar$		(7)

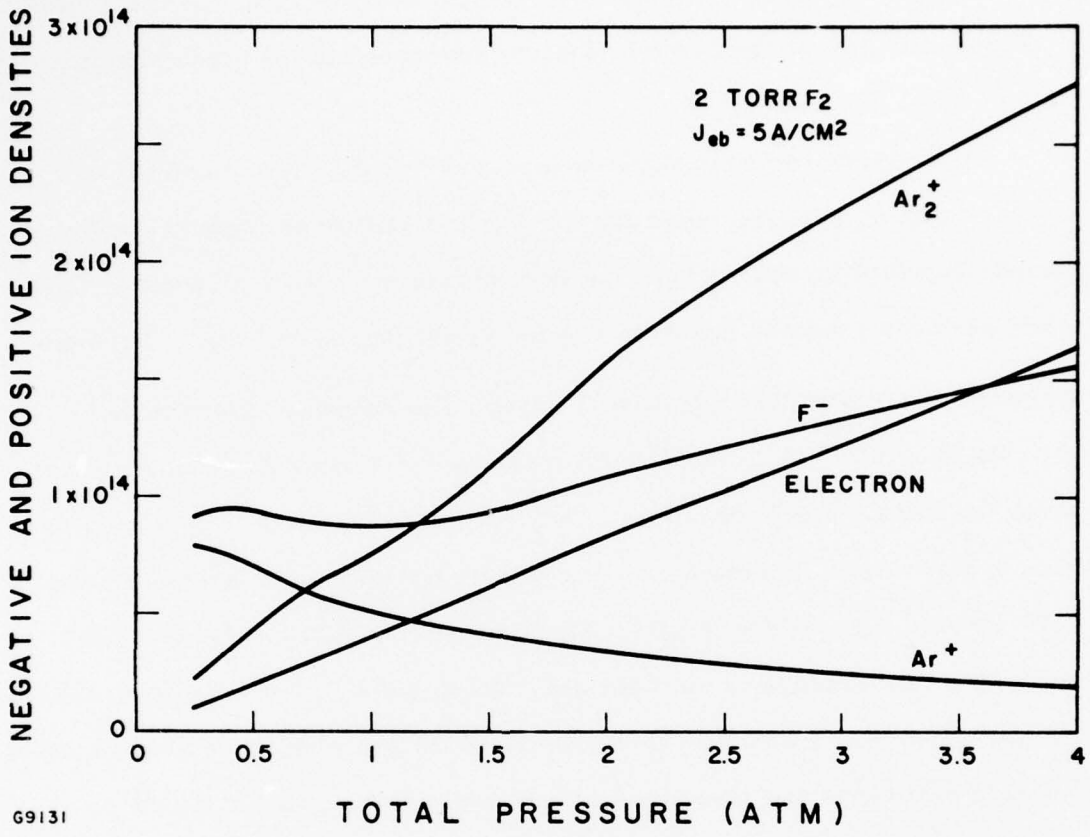

Figure 2 Calculated Densities of e_s, Ar^+, Ar_2^+ and F^- as a Function of Pressure in a Ar/F_2 Mixture Containing 2 Torr F_2

Ar^+ densities are nearly equal at an atmosphere. At 4 atmospheres the electron density is slightly greater than the F^- density. Even at these high pressures only 20% of the ArF* formation proceeds via the electron-ion recombination channel.

At pressures below an atmosphere ArF* is mainly formed via reaction (4). In this pressure range the ion-ion equivalent two body recombination rate constant increases linearly with pressure (3-body process). This 3-body reaction becomes diffusion limited at pressures > 1 atm. Between pressures of 1-4 atm this reaction is expected to reach an effective two-body rate of $\sim 10^{-6}$ cm^3/sec.[9] At pressures $\approx$ 1 atm, Ar_2^+ and Ar^+ have almost the same number densities. Ar_2^+ recombines with F^- via 2-body reaction to form ArF* (reaction 7). The molecular ions could possibly form Ar_2F^* via $Ar_2^+ + F^- + M \rightarrow Ar_2F^* + M$. However, it will be shown subsequently that this process is unimportant. Once ArF* is formed it can radiate or be quenched by F_2 or other constituents of the gas mixture. The dominant quenching processes and measured rate constants are listed in Table 2.

(b) Quenching of ArF*

A series of experiments were run with 2 torr of F_2 and varying Ar pressure from 60 torr to 1 atmosphere. The signal increased linearly to about 200 torr of Ar. As the e-beam power deposited into the mix increases linearly with the Ar partial pressure, this result shows that Ar quenching of ArF* is negligibly small at partial pressures of $\leq$ 200 torr.

We next observed the ArF* fluorescence keeping the Ar partial pressure fixed at 150 torr[10] and varying the F_2 partial pressure from 2-20 torr.

(9) M. R. Flannery, "Ionic Recombination" (unpublished).

(10) It was determined aposteriori that at 150 torr the Ar quenching of ArF* introduces a 5% error. This error was corrected for subsequently.

TABLE 2. DOMINANT QUENCHING PROCESSES OF ArF*

Reaction	(Rate Constant)x (ArF* Lifetime)	Rate Constant[a]
$ArF^* + F_2 \rightarrow$ Products	$7.6 \pm 0.7 \times 10^{-18}$ cm^3	1.9×10^{-9} cm^3/sec
$ArF^* + Kr \rightarrow KrF^* + Ar$	$6.1 \pm 0.5 \times 10^{-18}$ cm^3	1.6×10^{-9} cm^3/sec
$ArF^* + Ar \rightarrow$ Products	$3.6 \pm 1 \times 10^{-20}$ cm^3	9×10^{-12} cm^3/sec
$ArF^* + 2Ar \rightarrow Ar_2F^* + Ar$	$1.6 \pm 0.3 \times 10^{-39}$ cm^6	4×10^{-31} cm^6/sec

[a] The rate constants have been evaluated assuming an ArF* lifetime of 4 nsec.[10]

A Stern-Volmer plot of the ArF* fluorescence data as a function of the F_2 partial pressure is shown in Figure 3. From this plot, the half-pressure for F_2, i.e., the pressure of F_2 where the inverse quenching rate becomes equal to ArF* lifetime, is 4.0 torr.

To determine the quenching of ArF* by Ar, experiments were performed keeping the partial pressure of F_2 fixed at 2 torr and varying the partial pressure of Ar from 100 torr to 4 atm. Figure 4 shows the data for a typical set of runs. Notice that the signal increases up to a pressure of about one atmosphere and then decreases slowly.

There are two possibilities for the observed decay:

(1) ArF* quenching by Ar in two and three body processes, or

(2) Decreasing formation efficiency of ArF*

As the Ar pressure is increased, reaction (6) (in Table 1) occurs more frequently to form molecular ions Ar_2^+. In fact, from Figure 2, we see that at the highest pressure the density of Ar_2^+ is ten times that of Ar^+. These molecular ions will recombine with F^- and can form ArF* or possibly the excited triatomic Ar_2F^*. The formation of the Ar_2F^* by this channel will result in a smaller formation efficiency of ArF* and could account for the observed decrease in the fluorescence with increasing pressure. To ensure that this was in fact not the case, we attenuated the e-beam current by a factor of 25. This causes a decrease of the F^- density by at least a factor of 5, resulting in a higher probability of Ar_2^+ formation at a given pressure. So changing the current factor of 25 should strongly affect the fluorescence efficiency of ArF* if the Ar_2^+ plus F^- form Ar_2F^*. Figure 5 shows the experimentally determined ratio of the ArF* fluorescence intensity as a function of pressure

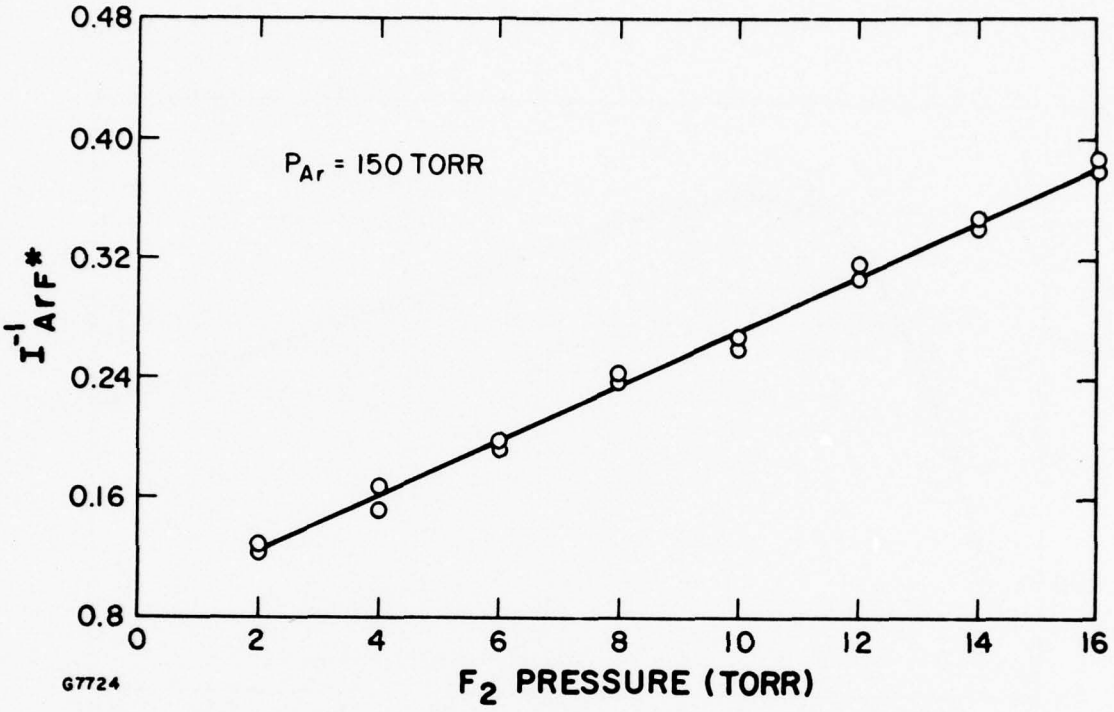

Figure 3 Stern-Volmer Quenching Curve for ArF^* ($^2\Sigma_{1/2}$) with F_2

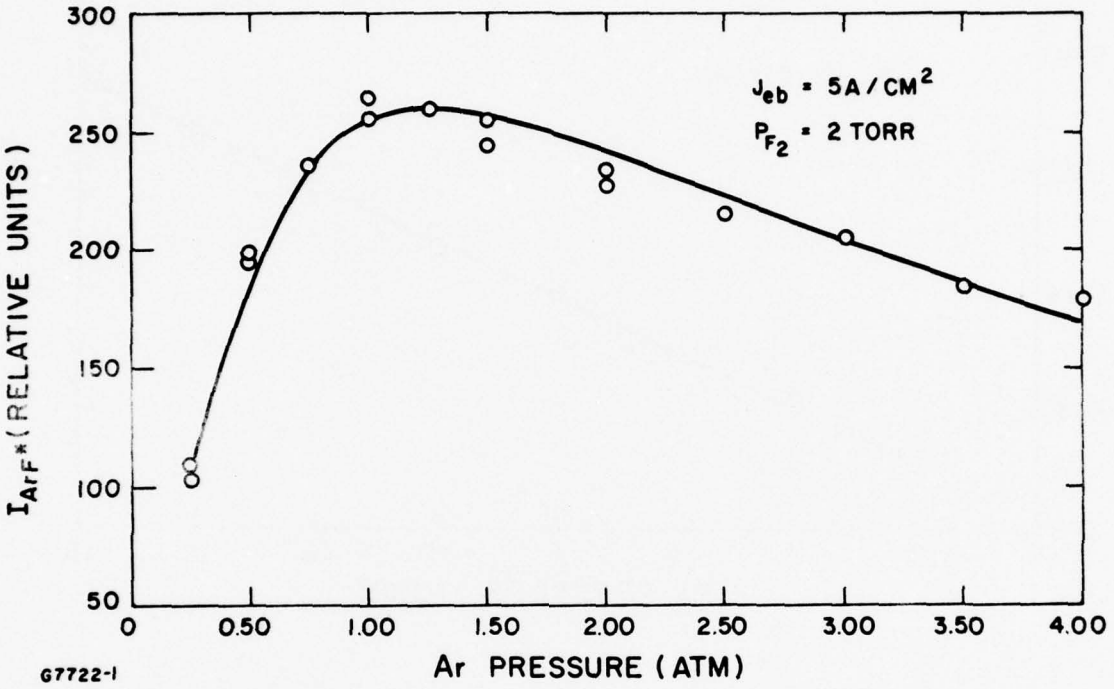

Figure 4 $ArF^* \, ^2\Sigma_{1/2} \rightarrow \, ^2\Sigma_{1/2}$ Fluorescence in the Presence of 2 Torr F_2 as a Function of Ar Partial Pressure. The points are experimental values for 5 A/cm^2 e-beam current. The curve is the expected ArF^* fluorescence using the measured quenching rate constants.

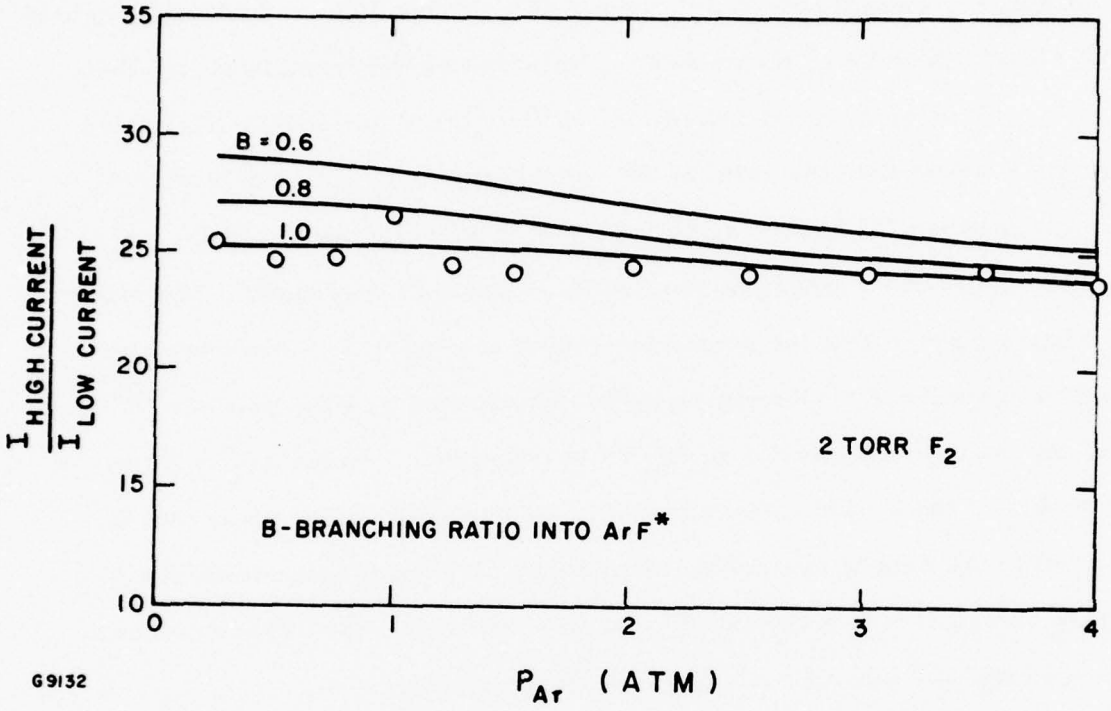

Figure 5 The Measured and Calculated Ratio of ArF^* Fluorescence Intensities When the E-Beam Current is Changed by a Factor of 25. The points are experimental. The three curves are the calculated ratios for branching ratios of 1, 0.8 and 0.6.

when the e-beam current is changed by a factor of 25. Also show are predicted ratios for three cases: (1) 100% of Ar_2^+ forms ArF*, (2) 80% of Ar_2^+ forms ArF*, and (3) 60% of Ar_2^+ form ArF*. From Figure 5 we can conclude that almost all the Ar_2^+ forms ArF*. Note that as the fraction of Ar_2^+ that forms ArF* decreases, the predicted ratio of the fluorescence intensities becomes larger than the ratio of the corresponding e-beam currents (25). This is because for branching ratios[11] < 1, losses resulting from Ar_2^+ formation become more important as the current is decreased. The results in Figure 5 prove that the dominant product of ($Ar_2^+ + F^-$) recombination is ArF* and not Ar_2F^*. Recent ab initio calculations by Wadt and Hay[12] show that the stable configuration of Ar_2F^* is triangular. So for $Ar_2^+ + F^-$ to form Ar_2F^* the F^- ion trajectory has to be contained in the plane that is normal to the axis of symmetry. Any other trajectory will result in a strong interaction between the F^- and Ar^+ and reduce the attractive force between the Ar^+ and Ar resulting in ArF* formation.

As a result of the experimental results and calculations shown in Figure 5 one can conclude that the decrease in the fluorescence amplitude with increasing Ar pressure is caused by quenching of ArF* by Ar. So the ArF* fluorescence signal S can be written as

$$S = \frac{\alpha N_{Ar}}{1 + (k_{F_2} N_{F_2} + k_{Ar} N_{Ar} + k_{2\,Ar} N_{Ar}^2)\tau} \qquad (1)$$

where α is a constant, τ is the ArF* radiative lifetime, k_{F_2} is the quenching rate constant of ArF* by F_2, k_{Ar} and k_{2Ar} are the two and three body quenching

(11) By branching ratio we mean the fraction of Ar_2^+ that forms ArF*.

(12) Willard R. Wadt and P. Jeffrey Hay, "The Low-Lying Electronic States of Ar_2F," Appl. Phys. Lett. 30, 573-575 (1977).

rate constants of ArF* by Ar. N_{F_2} and N_{Ar} are the number densities of F_2 and Ar respectively. We have ignored the three body quenching of ArF* by F_2 because of the low concentration (2 torr) of F_2 used. For example, a three body rate constant of 10^{-30} cm^6/sec for F_2 would change the results by $\leq$ 10%. Analysis of Eq. (1) to obtain the $k\tau$ products has been discussed in detail previously.[7] The curve in Figure 4 is a plot of Eq. (1) using the quenching rate constants obtained by that analysis.

Figure 6 shows the Ar_2F^* fluorescence amplitude as a function of Ar pressure. Since ArF* is formed first, we postulate that Ar_2F^* is formed by the following reaction

$$ArF^* + 2Ar \rightarrow Ar_2F^* + Ar$$

As evidence of this thesis, the shape of the Ar_2F^* fluorescence amplitude versus Ar pressure has been calculated assuming ArF* is formed first and subsequently recombines with Ar to form Ar_2F^*. The result of this calculation is shown as the solid curve plotted in Figure 6. The deviation of the experimental data from the curve at high pressures is probably due to the quenching of Ar_2F^* by Ar.

(c) Displacement Reaction

The rate constant for the displacement reaction Kr + ArF* $\rightarrow$ KrF* + Ar was obtained by observing the decay of the steady state fluorescence intensity at 1930 Å as the partial pressure of Kr was increased. These measurements were made in mixes containing a constant amount of Ar and F_2. The argon partial pressure was 100 torr to minimize the formation of Ar_2^+ (see Figure 2). In fact, at this low pressure and for an e-beam current of 5 A/cm^2 we have numerically evaluated that Ar^+ is about an order of magnitude greater

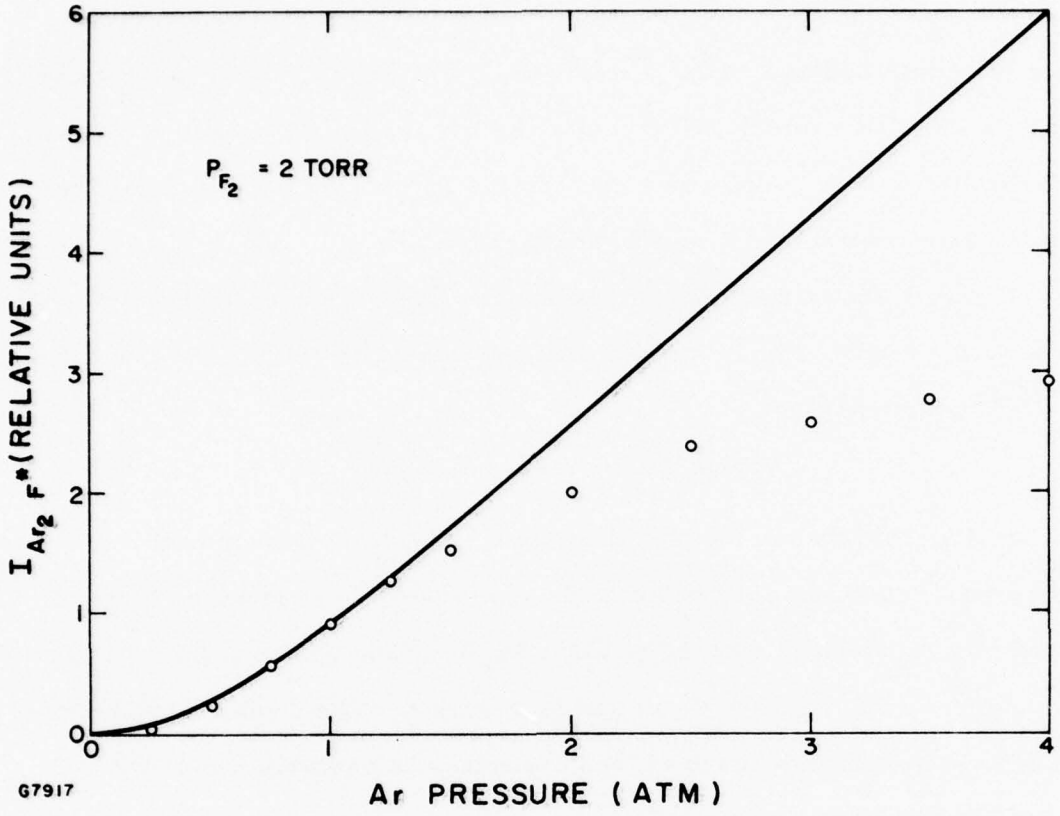

Figure 6 The Ar_2F^* Fluorescence in the Presence of 2 Torr as a Function of Ar Partial Pressure. The curve is the predicted Ar_2F^* fluorescence for negligible quenching of Ar_2F^*.

than Ar_2^+. Figure 7 shows the predicted decays of ArF* for our experimental conditions for two cases: (1) ignoring the Ar^+ channel; (2) including the Ar_2^+ channel; the Ar_2^+ channel introduces a variation of about 10% in this comparison. Figure 8 shows a Stern-Volmer plot of the ArF* fluorescence data as a function of the Kr partial pressure. From these plots we obtain the half quenching pressure of ArF* by Kr. The displacement reaction rate constant was also measured by observing the increase in the KrF* fluorescence amplitude with increasing Kr partial pressure. This measurement gives the same rate constant to within 10%, so one can conclude that Kr displaces ArF* to form KrF* with a branching ratio near unity.

The radiative lifetime of ArF* has been calculated to be 4 ns by Dunning and Hay.[13] Such a short lifetime gives a displacement rate constant (Kr + ArF* → KrF* + Ar) of 1.6×10^{-9} cm^3. This rate constant seems unusually large even for this sort of reaction. For example, the kinetically similar alkali-halide reaction Rb + KF → RbF + K has a rate constant about an order of magnitude smaller than these rare gas halide displacement reactions.[14] One reason for the difference may be related to the much higher exothermicity of the rare gas halide displacement reactions.[15] Another possible explanation for the rapid displacement rate constant is that at low pressure the Kr atom displaces the Ar atom when the ArF* is in a high vibrational level and thus has a large cross section.

(13) Thom. H. Dunning and P. Jeffrey Hay, "Electronic States of KrF," Appl. Phys. Lett. 28, 649-651 (1976).

(14) S. Stolte, A.E. Proctor and R.B. Bernstein, "Translational Energy Dependence of the Branching Fraction and Cross Sections for the Decay of Collision Complexes: K + CsF, RbF*," J. Chem. Phys. 65, 4990 (1976).

(15) M. Krauss, N.B.S., (private communication).

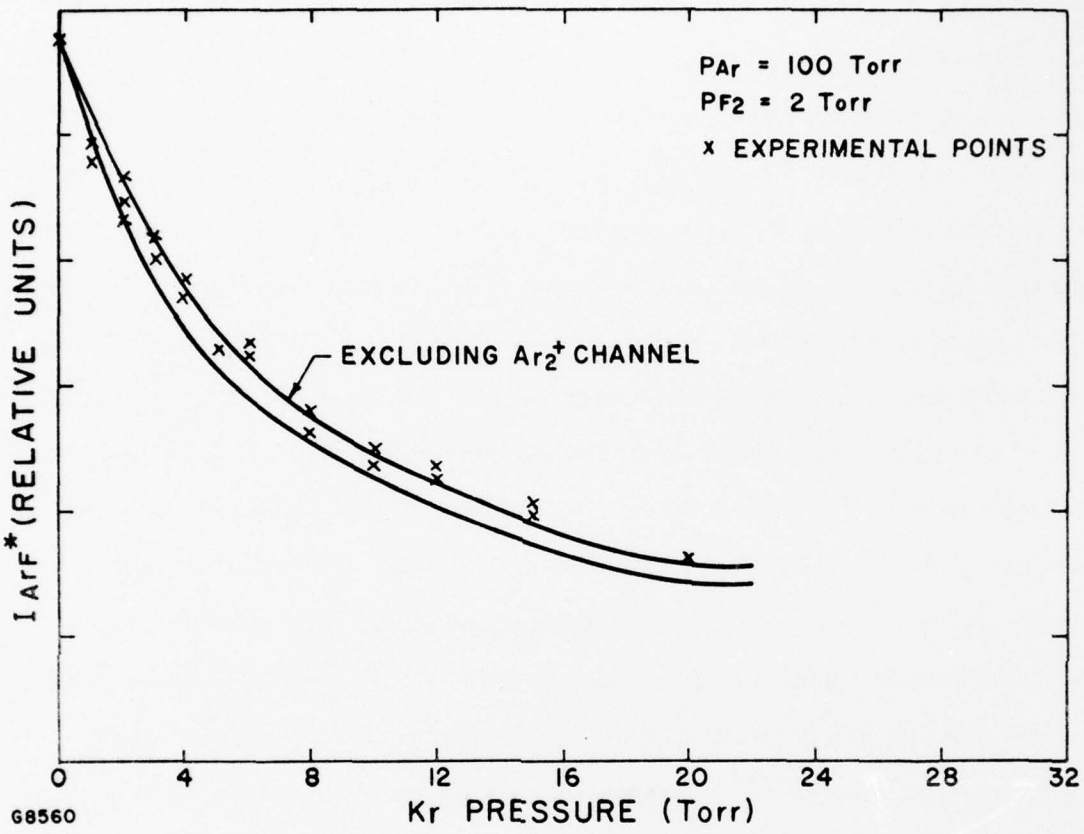

Figure 7 The Predicted and Measured ArF^* Fluorescence as a Function of the Kr Partial Pressure. When the charge transfer channel is excluded the predicted decay of the ArF^* signal as a function of Kr pressure is about 10% slower.

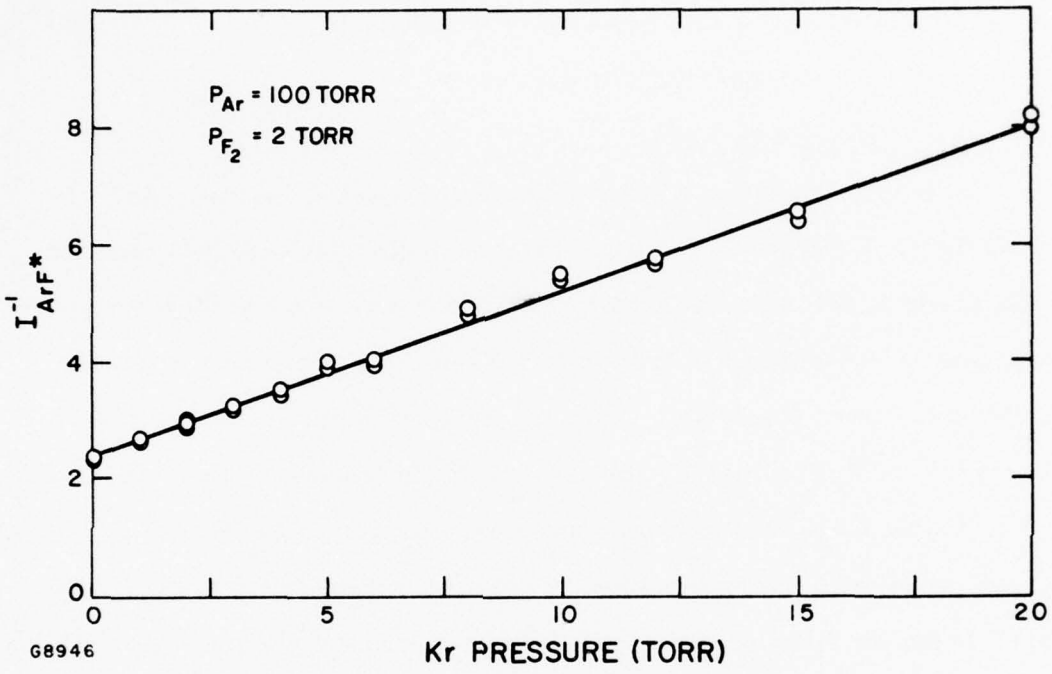

Figure 8 Stern-Volmer Quenching Curve for ArF^* with Kr

At higher pressures the vibrational relaxation of ArF* will proceed more rapidly. Therefore, one might expect the measured displacement rate to decrease with increasing pressure. Preliminary measurements at 200 and 300 torr Ar indicate that this indeed may be the case.

4. FORMATION AND QUENCHING OF KrF*

(a) Formation of KrF*

In mixtures containing mainly Ar at low total pressures, ArF* is formed first. KrF* is subsequently formed by the displacement reaction as discussed in the previous section. At pressures of about an atmosphere and greater (depending on e-beam current density), molecular argon ion formation becomes important. The Ar_2^+ rapidly charge transfers with Kr to form Kr^+.[16] For lean Kr mixes the Kr^+ recombines with F^- to form KrF*. As the Kr partial pressure and total mixture pressure are increased, Kr_2^+ will be formed. By experimental measurements similar to those discussed in the previous section, we have shown that Kr_2^+ recombines with F^- to form mainly KrF*. Once KrF* is formed it can radiate or be quenched by the constituents of the gas mixture. The dominant quenching processes and reaction rates are listed in Table 3.

(b) Quenching of KrF*

The rate constant for quenching of KrF* by F_2 was measured by observing the KrF* fluorescence amplitude versus pressure in binary mixtures of Kr and F_2. The procedure was similar to the measurements of ArF* quenching by F_2 described in the previous section. The two-body quenching of KrF^* by Kr and the three body quenching by 2Kr were studied in Kr/F_2 mixes, similar to the analogous case of ArF^* quenching by Ar as discussed in the previous section.

(16) D.K. Bohme, N.G. Adams, M. Moselman, D.B. Dunkin and E.E. Ferguson, "Flowing Afterglow Studies of the Reactions of the Rare-Gas Molecular Ions He_2^+ Ne_2^+ and Ar_2^+ with Molecules and Rare-Gas Atoms," J. Chem. Phys. 52, 5094 (1970).

TABLE 3. DOMINANT QUENCHING PROCESSES OF KrF*

Reaction	$k\tau_R$(KrF*)	$k(\tau_R = 6.5$ nsec)	
$KrF^* + F_2 \rightarrow$ Products	5×10^{-18} cm^3	7.8×10^{-10} cm^3 sec^{-1}	(1)
$KrF^* + 2Kr \rightarrow Kr_2F^* + Kr$	4.4×10^{-39} cm^6	6.7×10^{-31} cm^6 sec^{-1}	(2)
$KrF^* + Kr \rightarrow$ Products	$\leq 1.1 \times 10^{-20}$ cm^3		(3)
$KrF^* + Kr + Ar \rightarrow Kr_2F^* + Ar$	4.2×10^{-39} cm^6	6.5×10^{-31} cm^6 sec^{-1}	(4)
$KrF^* + 2Ar \rightarrow$ Products	4.6×10^{-40} cm^6	7×10^{-32} cm^6 sec^{-1}	(5)

Figure 9 shows the spontaneous emission spectra in mixtures containing 0.3% F_2, 6% Kr and 93.7% Ar at various total pressures. The uncalibrated spectral intensity scale is approximately logarithmic. At 0.5 atmosphere essentially all of the radiation from the mixture is contained in the KrF* $^2\Sigma_{1/2} \rightarrow {}^2\Sigma_{1/2}$ band at 248 nm. However, two other broad bands, containing much less energy, are observable. The first is centered at 415 nm and has been identified with the $^2B_2 \rightarrow A_1$ transition of the excited triatomic Kr_2F^*.[17] The other broad band, centered roughly at 270-280 nm, is most likely a combination of radiation from the $^2\Sigma$-$^2\Pi$ band of KrF* and perhaps radiation from the excited triatomics Ar_2F^*[18] and ArKrF*. Identification of the Kr_2F^* and Ar_2F^* bands was inferred by observing the radiation from binary mixtures of Ar/F_2 and Kr/F_2. From the Kr/F_2 mix we observed the same spectra excpet that some of the structure in the band centered at 270-280 nm disappeared. From the Ar/F_2 mixture, the spectra showed only a very broad band centered at 290-300 nm which has been identified as Ar_2F^* radiation. The spectrum obtained at a total mixture pressure of 4 atm indicates that, compared with the 0.5 atm spectrum, essentially the same energy is contained in the KrF* $^2\Sigma_{1/2} \rightarrow {}^2\Sigma_{1/2}$ band, although the electron beam energy deposited increased by a factor of ~ 8. This spectrum indicates that most of the additional energy deposited by the e-beam was channeled to Kr_2F^*. This decrease in the KrF* fluorescence efficiency and increase in the Kr_2F^* fluorescence efficiency could be due to two possible effects:

(17) M. Krauss, N.B.S., (private communication).

(18) Hao-Lin-Chen, R.E. Center, Daniel W. Trainor and W.I. Fyfe, "Dissociative Attachment of Electrons to F_2," Appl. Phys. Lett. 30, 99 (1977).

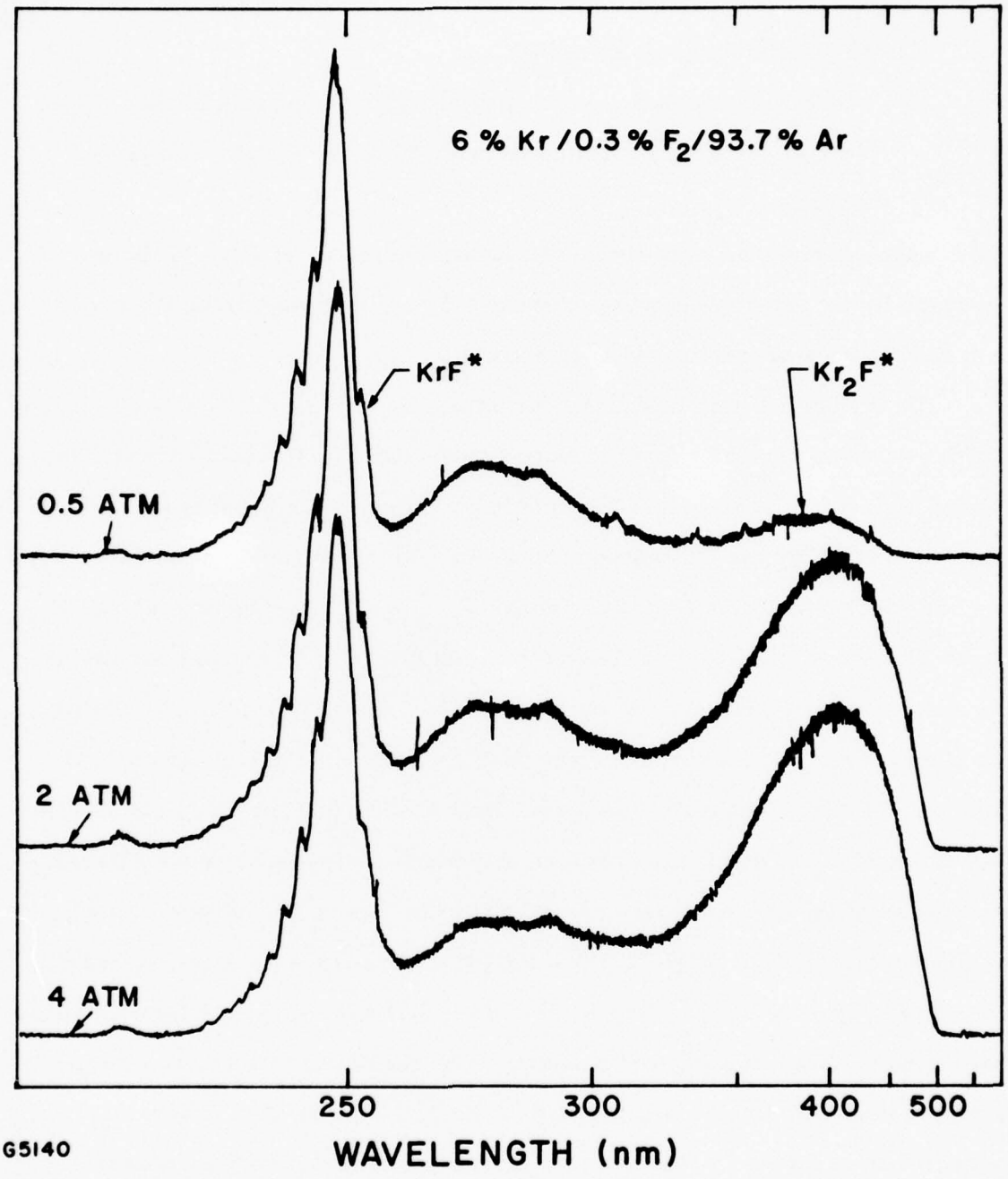

Figure 9 Spectra of a 6% Kr Mixture at Various Total Pressures

(1) KrF* quenching by Ar and Kr, or

(2) Decreasing formation efficiency of KrF*. Such a decrease is expected if Kr_2^+ recombines with F^- to form KrF* with a branching ratio < 1.

Experiments performed with different e-beam currents, similar to those discussed in the previous section, show that Kr_2 recombines with F^- to form KrF* with a branching ratio near unity.

To further substantiate this conclusion, an experiment was performed in which some of the KrF* formed were deactivated by stimulated transition induced by a KrF* laser before they could be collisionally quenched. If Kr_2F^* is formed by the quenching of KrF* as our measurements indicate, then stimulation of the KrF* transition ($B^2\Sigma_{1/2} \rightarrow X^2\Sigma_{1/2}$) by intense radiation at 249 nm should lead to a decrease in the Kr_2F^* fluorescence amplitude. The experimental set-up for the measurement is shown in Figure 10. Radiation from a KrF* TEA laser was transmitted along the length of the cell containing a KrF* laser mixture. The side light emission at 249 nm band (KrF*) and 410 nm (Kr_2F^*) were monitored by photodiodes with appropriate filters. The results of these measurements are shown in Figure 11. Figures 11(a) and (b) display the KrF* and Kr_2F^* sidelight fluorescence upon introduction of the KrF* laser pulse. Figure 11(c) shows the Kr_2F^* sidelight fluorescence when no KrF* laser radiation is present. The results of this set of experiments confirm that Kr_2F^* is a product of the KrF* quenching. Therefore, the decrease of the KrF* fluorescence efficiency with increasing pressure is a result of quenching by Ar and Kr.

The quenching of KrF* by processes (4) and (5) in Table 3 were studied in $Ar/Kr/F_2$ mixtures. Reaction (5) was determined by analyzing

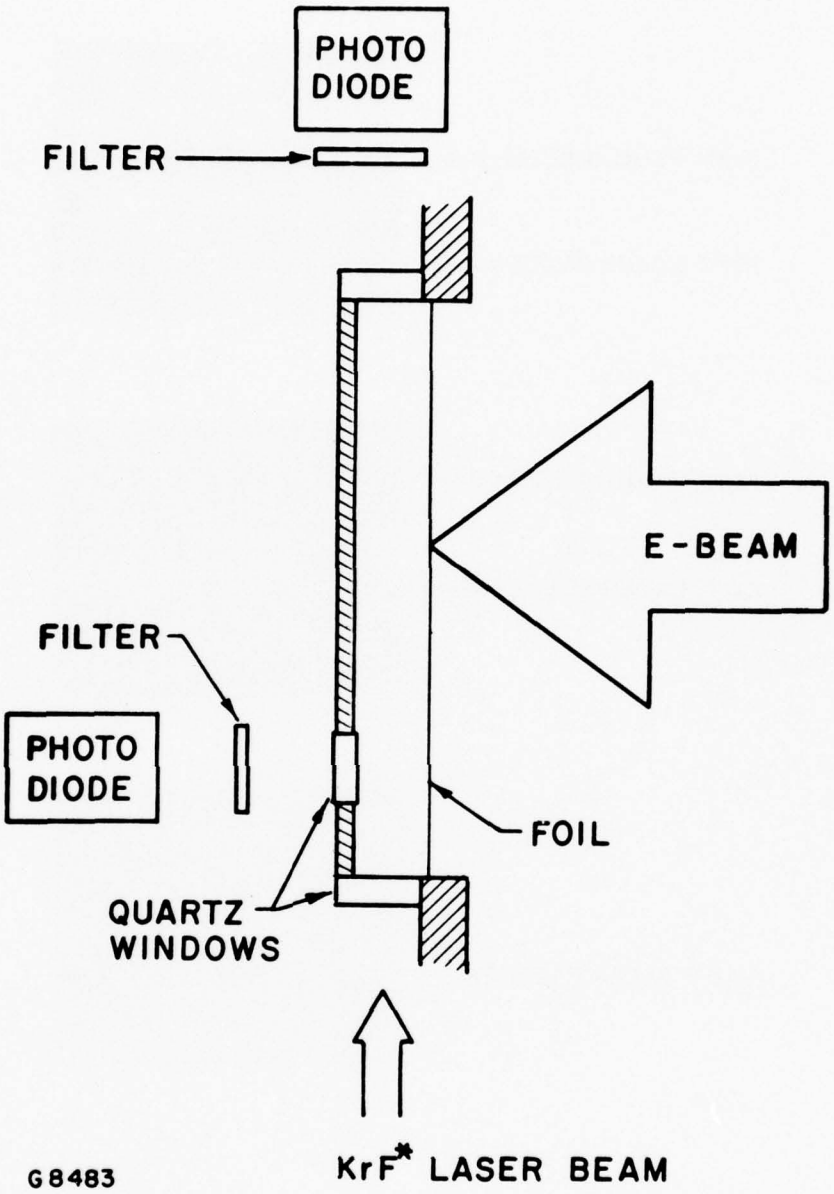

Figure 10 Experimental Set-Up for the KrF^* and Kr_2F^* Saturation Experiments

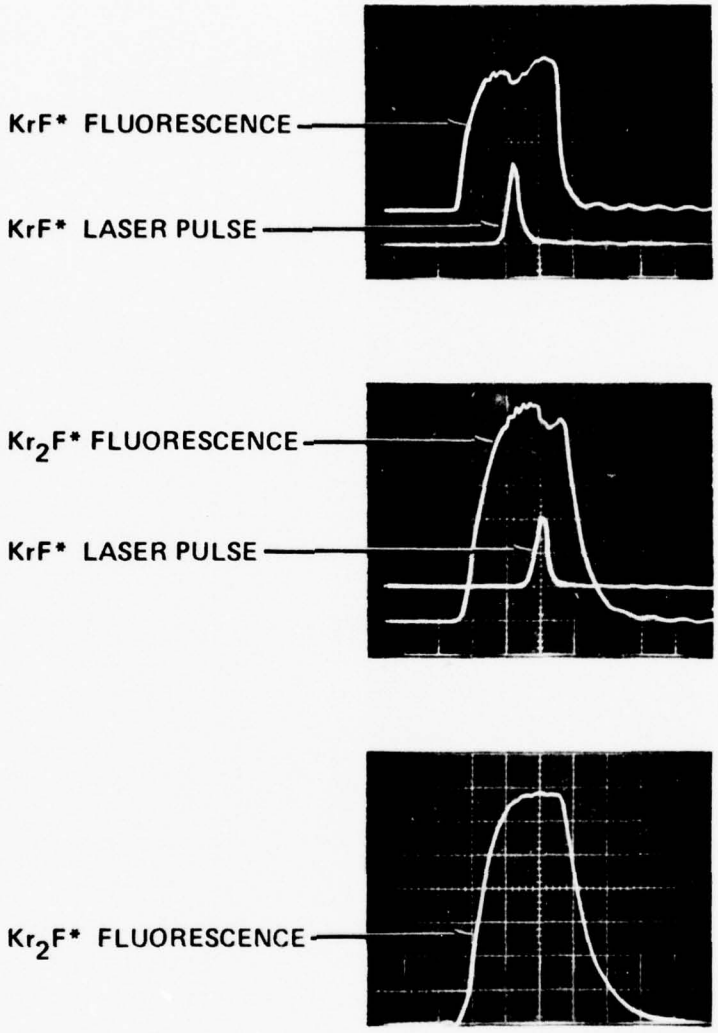

Figure 11 Data Showing the KrF^* and Kr_2F^* Fluorescence in the Presence of KrF^* Laser Radiation. The bottom oscillogram is the Kr_2F^* fluorescence when there is no laser radiation present.

the dependence of the KrF* fluorescence on the Ar partial pressure. The F_2 and Kr partial pressures were kept constant for these runs. For such a mix reaction (4) appears as an effective two-body reaction (Kr constant). Because of their different pressure dependence, two and three body processes can be differentiated by an analysis similar to that discussed in detail in Ref. (19).

To measure reaction (4) more accurately, the KrF* fluorescence intensity as a function of the Kr partial pressure was measured. In these measurements the Ar and F_2 partial pressures were kept constant. Figure 12 shows typical data for the KrF* fluorescence intensity as a function of Ar partial pressure. The curves represent the predicted pressure dependence of the KrF* intensity using the rate constants in Table 3.

5. CONCLUSION

In the preceding sections we have shown that the ArF* and KrF* exciplexes can be formed via the ion channel with unit branching. From our measurements we can conclude that the decrease of the fluorescence intensity with increasing pressure is a result of two and three body quenching of the exciplex.

Interception of the precursors (Ar^+, Kr^+ and F^-) of these exciplexes are a negligibly small effect when the experimental conditions are chosen properly. In a laser it is possible to minimize the loss due to the quenching processes by saturating the lasing transition. We have identified the dominant quenching processes of ArF* ($B^2\Sigma_{1/2}$) and KrF* ($B^2\Sigma_{1/2}$) and measured their rate constants. The only important two body quenching is due to F_2.

(19) E.W. McDaniel, V. Cermak, A. Dalgarno, E.E. Ferguson and L. Friedman, "Ion-Molecule Reactions," (Wiley-Interscience, New York, 1970) pp. 338-339.

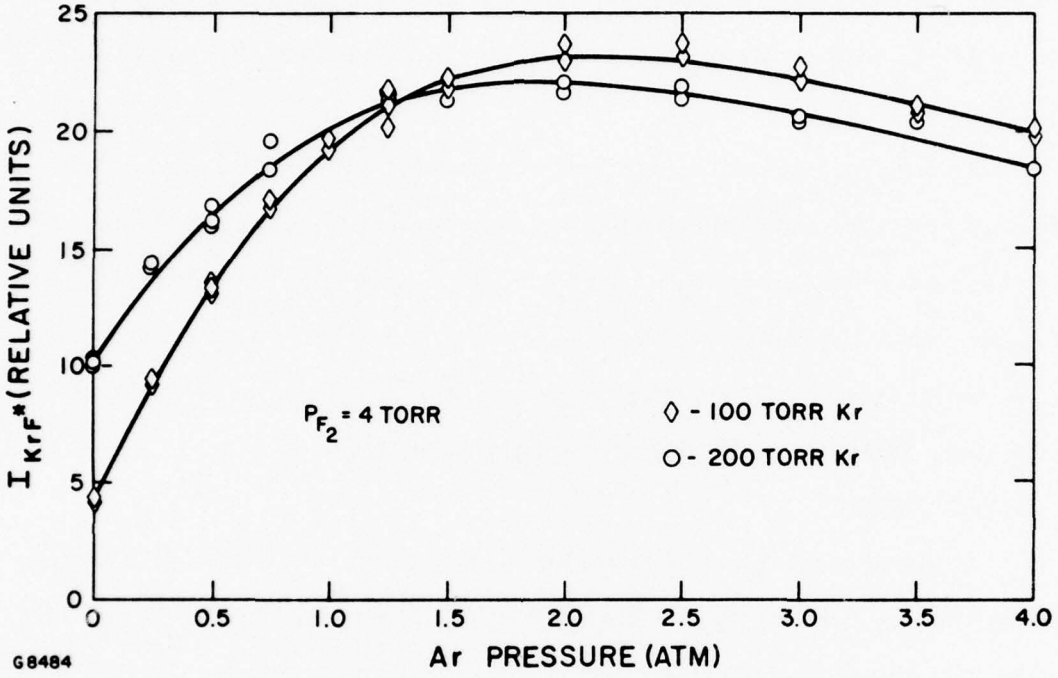

Figure 12 KrF^* Fluorescence Signal for $Ar/Kr/F_2$ Mixtures Containing 4 Torr F_2 and 100 and 200 Torr Kr. The data was taken varying only the Ar partial pressure. The curves are the calculated fluorescence using the rate constants listed in Table 3.

Three body quenching by the rare gases becomes important at pressures above one atmosphere. These quenching processes result in the formation of excited triatomics Ar_2F^* and Kr_2F^*. The formation of the excited triatomics can be understood by looking at the schematic potential curves shown in Figure 13. The rare gas R approaches the rare gas fluoride, RF*, on a repulsive curve that intersects the $R_2^+F^-$ potential curve. The surface of the interaction will be dependent of ΔE the exothermicity of the interaction. The larger ΔE the larger the surface area and hence the interaction will proceed with a higher probability. According to Wadt and Hays[12] calculation $\Delta E \approx 0.6$ eV for Ar_2F^* and Kr_2F^*. For Xe_2F^*, ΔE is only 0.2 eV. This small exothermicity might be responsible for the fact that Xe_2F^* has not been observed. From the spontaneous emission spectra and the measured quenching rate constants the saturation flux can be calculated for a particular mixture. This information, coupled with the knowledge of the photoabsorption of the active medium, can be used to optimize laser mixes.

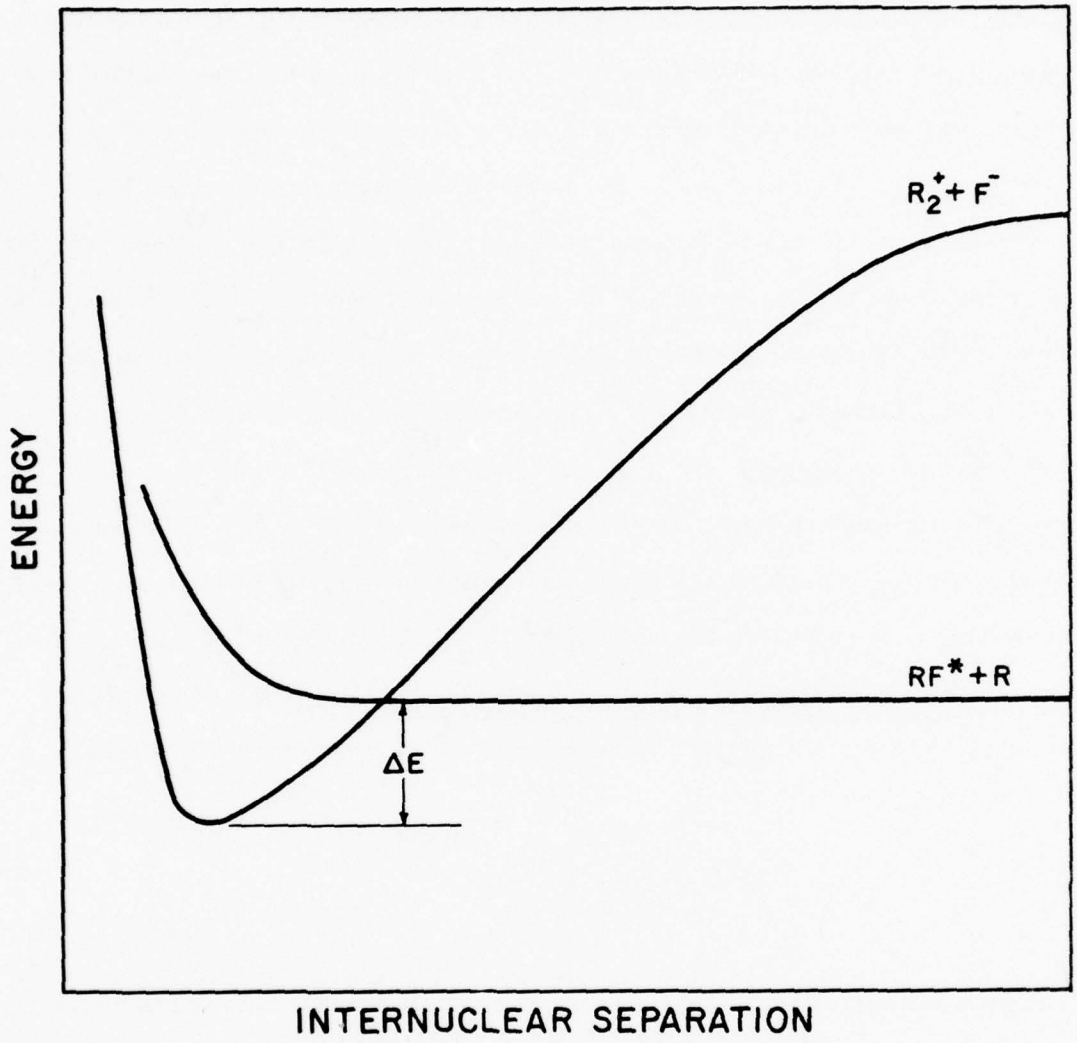

Figure 13 Schematic of Potential Curves of $R_2^+ + F^-$ and $RF^* + R$

REFERENCES

1. J.E. Velazco and D.W. Setser, "Quenching of the Xe Metastable Atoms," JQE 11, 708-709 (1975).

2. J.J. Ewing and C.A. Brau, "Laser Action on the $^2\Sigma^+_{1/2} \rightarrow {}^2\Sigma^+_{1/2}$ Bands of KrF and XeCl," Appl. Phys. Lett. 27, 350-352 (1975).
C.A. Brau and J.J. Ewing, "354 nm Laser on XeF," Appl. Phys. Lett. 27, 435-437 (1975).
S.K. Searles and G.A. Hart, "Stimulated Emission at 281.8 nm from XeBr," Appl. Phys. Lett. 27, 243-245 (1975).
E.R. Ault, R.S. Bradford and M.L. Bhaumik, "High Power Xenon Fluoride Laser," Appl. Phys. Lett. 27, 413-415 (1975).

3. J.A. Mangano and J.H. Jacob, "Electron Beam Controlled Discharge Pumping of KrF Laser," Appl. Phys. Lett. 27, 495-497 (1975).
R. Burnham, H.W. Harris and N. Djeu, "Xenon Fluoride Laser Excitation by Transverse Electric Discharge," Appl. Phys. Lett. 28, 86-87 (1976).
C.P. Wang, H. Mirels, D.G. Sutton and S.N. Suchard, "Fast Discharge Initiated XeF Laser," Appl. Phys. Lett. 28, 326-328 (1976).
J.A. Mangano, J.H. Jacob and J.B. Dodge, "Electron-Beam-Controlled Discharge Pumping of the XeF Laser," Appl. Phys. Lett. 29, 426-428 (1976).

4. J.A. Mangano, et al, "An 8.5 Liter E-beam Pumped KrF* Laser," (unpublished).

5. R Hunter (unpublished).

6. J.E. Velazco, J.H. Kolts and D.W. Setser, "Quenching Rate Constants for Metastable Argon, Krypton, and Xenon Atoms by Fluorine Containing Molecules and Branching Ratios of XeF* and KrF* Formation," J. Chem. Phys. 65, 3468-3485 (1976).

7. M. Rokni, J.H. Jacob, J.A. Mangano and R. Brochu, "Two and Three Body Quenching of XeF* by Ar and Xe," Appl. Phys. Lett. 30, 458-460 (1977).

8. L.R. Peterson and J.E. Allen, Jr., "Electron Impact Cross Sections for Argon," J. Chem. Phys. 56, 6068-6076 (1972).

9. M.R. Flannery, "Ionic Recombination" (unpublished).

10. It was determined aposteriori that at 150 torr the Ar quenching of ArF* introduces a 5% error. This error was corrected for subsequently.

11. By branching ratio we mean the fraction of Ar_2^+ that forms ArF*.

12. Willard R. Wadt and P. Jeffrey Hay, "The Low-Lying Electronic States of Ar_2F," Appl. Phys. Lett. 30, 573-575 (1977).

13. Thom. H. Dunning and P. Jeffrey Hay, "Electronic States of KrF," Appl. Phys. Lett. 28, 649-651 (1976).

14. S. Stolte, A.E. Proctor and R.B. Bernstein, "Translational Energy Dependence of the Branching Fraction and Cross Sections for the Decay of Collision Complexes: K + CsF, RbF*," J. Chem. Phys. 65, 4990 (1976).

15. M. Krauss, N.B.S., (private communication).

16. D.K. Bohme, N.G. Adams, M. Moselman, D.B. Dunkin and E.E. Ferguson, "Flowing Afterglow Studies of the Reactions of the Rare-Gas Molecular Ions He_2^+ Ne_2^+ and Ar_2^+ with Molecules and Rare-Gas Atoms," J. Chem. Phys. 52, 5094 (1970).

17. M. Krauss, N.B.S., (private communication).

18. Hao-Lin-Chen, R.E. Center, Daniel W. Trainor and W.I. Fyfe, "Dissociative Attachment of Electrons to F_2," Appl. Phys. Lett. 30, 99 (1977).

19. E.W. McDaniel, V. Cermak, A. Dalgarno, E.E. Ferguson and L. Friedman, "Ion-Molecule Reactions" (Wiley-Interscience, New York, 1970), pp. 338-339.

APPENDIX A

FORMATION AND QUENCHING KINETICS OF ArF*

APPENDIX A

FORMATION AND QUENCHING KINETICS OF ArF*

Recently there has been considerable research into the formation and quenching kinetics of the excited states of the rare-gas halides.[1-7] Such information is necessary for designing a laser system based on these "exciplex" molecules and choosing the appropriate mixture. While ArF* is itself an interesting species for a laser capable of achieving large output energy,[8] it is also a "precursor" for the KrF* and XeF* lasers.[4, 6] This is because the KrF and XeF laser mixes contain $\geq$ 90% Ar. Consequently most of the e-beam power deposited into the gas ends up as Ar^+ or Ar*. These excited states react with F^- and F_2 to form ArF*. The argon atom in ArF* is then displaced by Kr or Xe to form KrF* or XeF*.

Formation of ArF* and KrF* for studies of their quenching kinetics is complicated by the fact that these molecules have unstable ground states.

(1) A. Hawryluk, J.A. Mangano, and J.H. Jacob, 3rd Summer Colloquium on Electronic Transition Lasers, 1976 (unpublished).

(2) D.C. Lorents, R.M. Hill, D.L. Huestis, M.V. McCusker, and N.H. Nakano, in Ref. 1.

(3) J.E. Velazco, J.H. Kolts and D.W. Setser, J. Chem. Phys. 65, 3468 (1976).

(4) J.A. Mangano, J.H. Jacob, M. Rokni, and A. Hawryluk, Appl. Phys. Lett. 31, 26 (1977).

(5) H.C. Brashears, Jr., D.W. Setser, and D. MesMarteau (unpublished).

(6) M. Rokni, J.H. Jacob, J.A. Mangano, and R. Brochu, Appl. Phys. Lett. 30, 458 (1977).

(7) D.W. Setser (private communication).

(8) J.M. Hoffman, A.K. Hays, and G.C. Tisone, Appl. Phys. Lett. 28, 538 (1976).

A convenient way, which we utilize in this work, for generating these excimers is by irradiating the relevant mixtures with fast electrons. In this letter we report on the formation, quenching, and displacement kinetics of ArF*.

The kinetic channels and quenching rates are determined by analyzing the dependence of the ArF* ($^2\Sigma_{1/2} \rightarrow {}^2\Sigma_{1/2}$) fluorescence intensity as a function of pump power, mixture ratio, and pressure. Broad-band emission centered at 290 nm, which has been attributed to Ar_2F^* emission,[9] has been observed. Our data strongly indicates that the Ar_2F^* is formed by a three-body recombination of ArF* with Ar. We have determined the product of the rate constants k and ArF* radiative lifetime[10] τ for the processes listed in Table A-1. In measuring these rate constants care was taken to discriminate and isolate the reaction of interest. The high-energy e-beam apparatus used for the excitation of the gas mixture has been described previously.[11] The ArF* fluorescence was detected by passing the 1930-Å radiation through two 250-Å bandpass filters. The second filter was coated with a solution of sodium silicitate that fluoresced in the visible. This fluorescence was assumed to be proportional to 1930-Å radiation impinging onto it. The visible fluorescence was detected by a photodiode. The e-beam pulse was 300 ns long. The observed fluorescence at 1930 Å reached steady state, thereby simplifying the analysis of the data.

As we use Ar and F_2 in all the experiments, the first objective is to determine the quenching of ArF* by F_2 and Ar. A series of experiments

(9) M. Krauss (private communication).

(10) T. H. Dunning and P. J. Hay, 7th Winter Colloquium on High Power Visible Lasers, Park City, Utah, 1977 (unpublished).

(11) J. A. Mangano and J. H. Jacob, Appl. Phys. Lett. 27, 495 (1975).

TABLE A-1. DOMINANT QUENCHING KINETICS OF ArF*

Reaction	(Rate Constant) x (ArF* Lifetime)	Rate Constant[a]
$ArF^* + F_2 \rightarrow$ Products	$7.6 \pm 0.7 \times 10^{-18}$ cm^3	1.9×10^{-9} cm^3/sec
$ArF^* + Kr \rightarrow KrF^* + Ar$	$6.1 \pm 1.5 \times 10^{-18}$ cm^3	1.6×10^{-9} cm^3/sec
$ArF^* + Xe \rightarrow XeF^* + Ar$	$1.8 \pm 0.2 \times 10^{-17}$ cm^3	4.5×10^{-9} cm^3/sec
$ArF^* + Ar \rightarrow$ Products	$3.6 \pm 1 \times 10^{-20}$ cm^3	9×10^{-12} cm^3/sec
$ArF^* + 2Ar \rightarrow Ar_2F^* + Ar$	$1.6 \pm 0.3 \times 10^{-39}$ cm^6	4×10^{-31} cm^6/sec

[a] The rate constants have been evaluated assuming an ArF* lifetime of 4 ns (Ref. 10).

were run with 2 torr of F_2 varying Ar pressure from 60 torr to 1 atm. The signal increased linearly to about 200 torr of Ar. As the e-beam power deposited into the mix increases linearly with the Ar partial pressure, this result shows that Ar quenching of ArF* is negligibly small at partial pressures of $\leq$ 200 torr.

We next observed the ArF* fluorescence, keeping the Ar partial pressure fixed at 150 torr[12] and varying the F_2 partial pressure from 2 to 20 torr. A Stern-Volmer plot of the ArF* fluorescence data as a function of the F_2 partial pressure is shown in Figure A-1. From this plot, the half-pressure of F_2, i.e., the pressure of F_2 where the inverse quenching rate becomes equal to the ArF* lifetime is 4.0 torr.

To determine the quenching of ArF* by Ar, experiments were performed keeping the partial pressure of F_2 fixed at 2 torr and varying the partial pressure of Ar from 100 torr to 4 atm. Figure A-2 shows the data for a typical set of runs. Note that the signal increases up to a pressure of about 1 atm and then decreases slowly.

There are two possibilities for the observed decay: (a) ArF* quenching by Ar or (b) a decrease in the formation efficiency of ArF*. Table A-2 lists the dominant formation kinetics for our experimental conditions.[13] As the Ar pressure is increased, reaction (4) proceeds with a higher probability to form molecular ions Ar_2^*. These molecular ions will recombine with F^- and can form either ArF* or the excited triatomic Ar_2F^*. The formation

(12) It was determined aposterion that at 150 torr the Ar quenching of ArF* introduces a 5% error. This error was corrected for subsequently.

(13) About 10% of the e-beam power goes directly into producing the rare-gas metastables. See for example, L. R. Peterson and J. E. Allen, J. Chem. Phys. 56, 6068 (1972). In the experiments performed the primary loss for Ar* is by F_2 quenching to form ArF*.

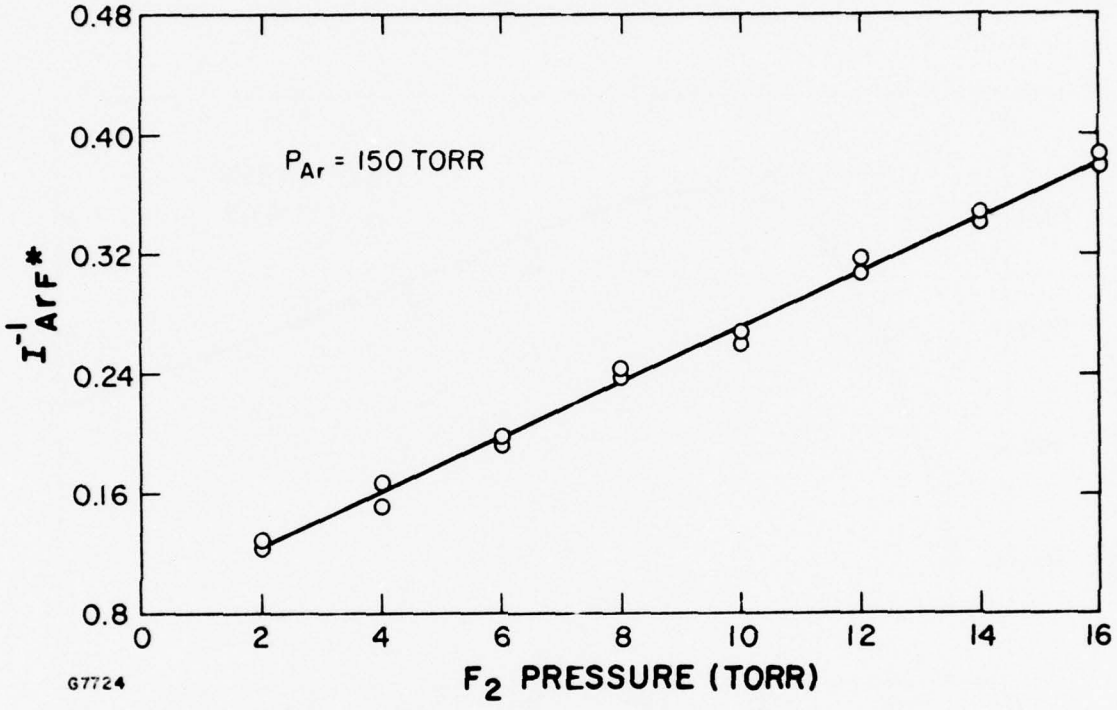

Figure A-1 Stern-Volmer Quenching Curve for ArF^* ($^2\Sigma_{1/2}$) With F_2

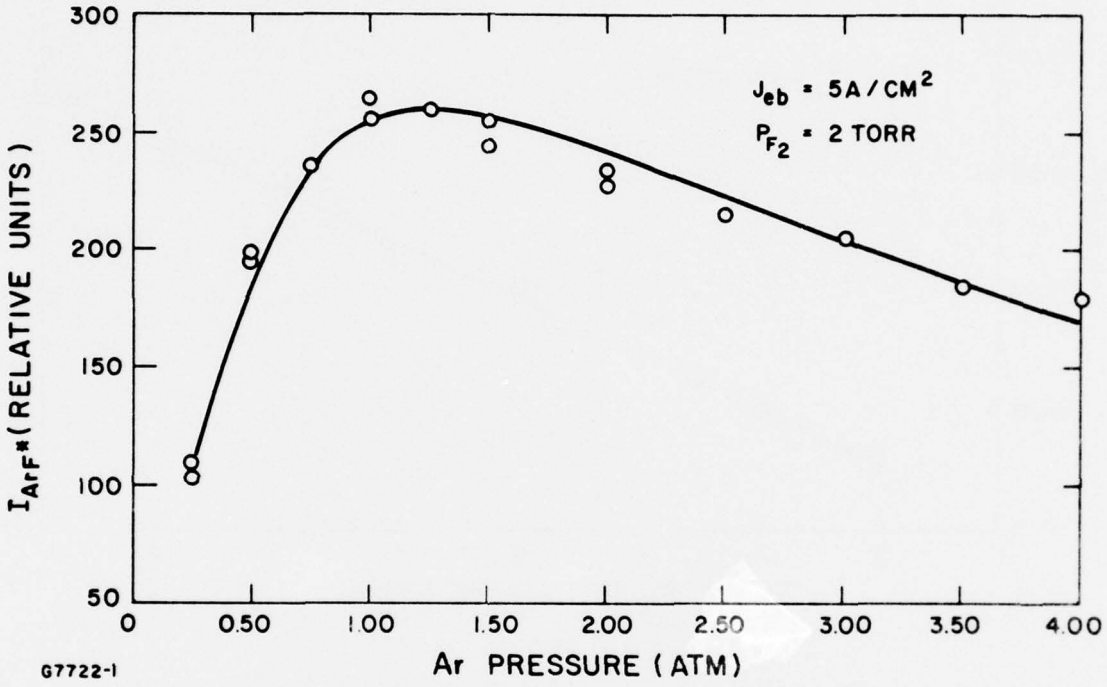

Figure A-2 $ArF^* \, ^2\Sigma_{1/2} \rightarrow \, ^2\Sigma_{1/2}$ Fluorescence, in the presence of 2 Torr F_2, as a Function of Ar Partial Pressure. The points are experimental values for 5 and 0.16 A/cm^2 e-beam current. The curve is the expected ArF^* fluorescence using the measured quenching rate constants.

TABLE A-2. DOMINANT FORMATION KINETICS FOR ArF*

$\vec{e} + Ar \rightarrow Ar^* + \vec{e} + e_s$	(1)
$e_s + F_2 \rightarrow F^- + F \quad 5 \times 10^{-9}\ cm^3/sec$[a]	(2)
$F^- + Ar^* + (M) \rightarrow ArF^* + (M)$	(3)
High Pressure	
$Ar^* + 2Ar \rightarrow Ar_2^* + Ar \quad 2.5 \times 10^{-31}\ cm^6/sec$[b]	(4)
$Ar_2^* + F^- \rightarrow ArF^* + Ar$	(5)

[a] Hao-Lin Chen, R.E. Center, Daniel W. Trainor, and W.I. Fyfe, Appl. Phys. Lett. 30, 99 (1977).

[b] E.W. McDaniel, V. Cermak, A. Dalgarno, E.E. Ferguson, and L. Friedman, Ion-Molecule Reactions (Wiley-Interscience, New York, 1970), p. 338.

of the Ar_2F^* by this channel will result in a smaller formation efficiency of ArF* and could account for the observed decrease in the fluorescence. To ensure that this was in fact not the case, we changed the e-beam current by a factor of 30. This causes a decrease of the F^- density of at least a factor of $(30)^{1/2}$ resulting in a higher probability of Ar_2^* formation at a given pressure. So changing the current by 30 should affect the decay of the ArF* fluorescence if the decrease is the result of an interference with the formation kinetics. The data in Figure A-2 shows the decay of ArF* is the same (within experimental scatter) for both low and high e-beam currents. For comparison the low-current fluorescence was multiplied by a constant factor. This result proves that the dominant product of $(Ar_2^* + F^-)$ recombination is ArF* and not Ar_2F^*. Hence the decrease in the fluorescence with increasing Ar pressure is because of quenching of ArF*. So the ArF* fluorescence signal S can be written

$$S = \frac{\alpha N_{Ar}}{1 + (k_{F_2} N_{F_2} + k_{Ar} N_{Ar} + k_{2Ar} N_{Ar}^2)\tau} \qquad (A-1)$$

where α is a constant, τ is the radiative lifetime, k_{F_2} is the quenching rate constant of ArF* by F_2, k_{Ar} and k_{2Ar} are the two- and three-body quenching rate constants of ArF* by Ar. N_{F_2} and N_{Ar} are the number densities of F_2 and Ar, respectively. We have ignored the three-body quenching of ArF* by F_2 because of the low concentration (2 torr) of F_2 used. For example, a three-body rate constant of 10^{-30} cm^6/sec for F_2 would change the results by $\leq$ 10%. Analysis of Eq. (A-1) to obtain the $k\tau$ products has been discussed in detail previously.[6] The curve in Figure A-2 is a plot of Eq. (A-1) using the quenching rate constants obtained by that analysis.

Figure A-3 shows the Ar_2F^* fluorescence as a function of the Ar pressure. We have argued earlier that $Ar_2^+ + F^-$ recombination predominantly forms ArF* rather than Ar_2F^*. Since ArF* is formed first, we postulate that Ar_2F^* is formed by the following reaction:

$$ArF^* + 2Ar \rightarrow Ar_2F^* + Ar.$$

As further evidence of this thesis, the curve in Figure A-3 is the formation of Ar_2F^* calculated assuming ArF* is formed first and subsequently recombines with Ar to form Ar_2F^*. The deviation of the experimental data from the curve at high pressures is probably due to the quenching of Ar_2F^* by Ar. From experimental observations of the temporal decay of the Ar_2F^* fluorescence, its radiative lifetime is of the order of 100 ns. Comparing Figures A-3 and A-4, this would imply that the Ar_2F^* quenching by Ar is at least an order of magnitude slower than the ArF* quenching by Ar.

The displacement rate constants of ArF* by Kr and Xe were obtained by observing the decay of the steady-state fluorescence intensity at 1930 Å as the partial pressure of Kr and Xe was increased. These measurements were made in mixes containing a constant amount of Ar and F_2. The argon partial pressure was low (P_{Ar} = 100 torr) to minimize the formation of Ar_2^+. In fact, at 100 torr Ar and for an e-beam current of 5 A/cm^2 we have numerically evaluated that Ar_2^+ is about an order of magnitude greater than Ar_2^+. These molecular ions rapidly charge transfer[14] to form Kr_2^+. Figure A-4 shows Stern-Volmer plots of the fluorescence data as a function of Kr and Xe partial pressures. From these plots we obtain the half quenching pressure of ArF* by Kr and Xe. The displacement reaction rates were

(14) D.K. Bohme, N.G. Adams, M. Moselman, D.B. Dunkin, and E.E. Ferguson, J. Chem. Phys. 52, 5094 (1970).

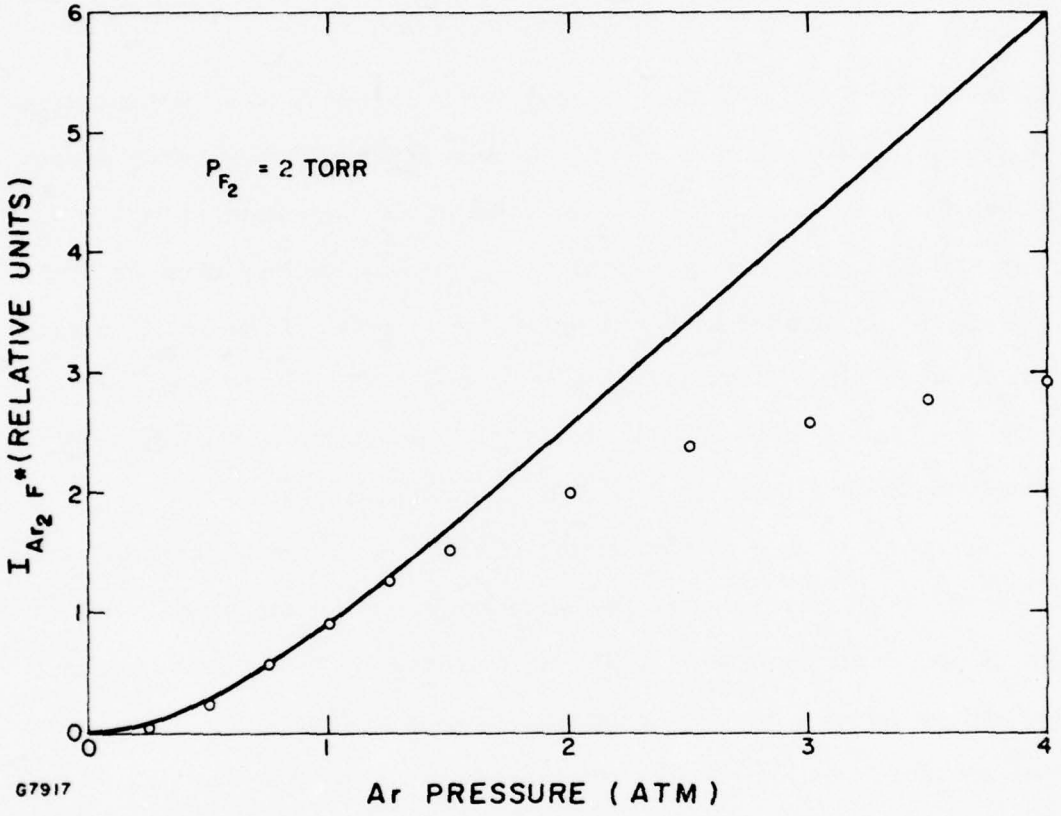

Figure A-3 The Ar_2F^* Fluorescence in the Presence of 2 Torr F_2 as a Function of Ar Partial Pressure. The curve is the predicted Ar_2F^* formation.

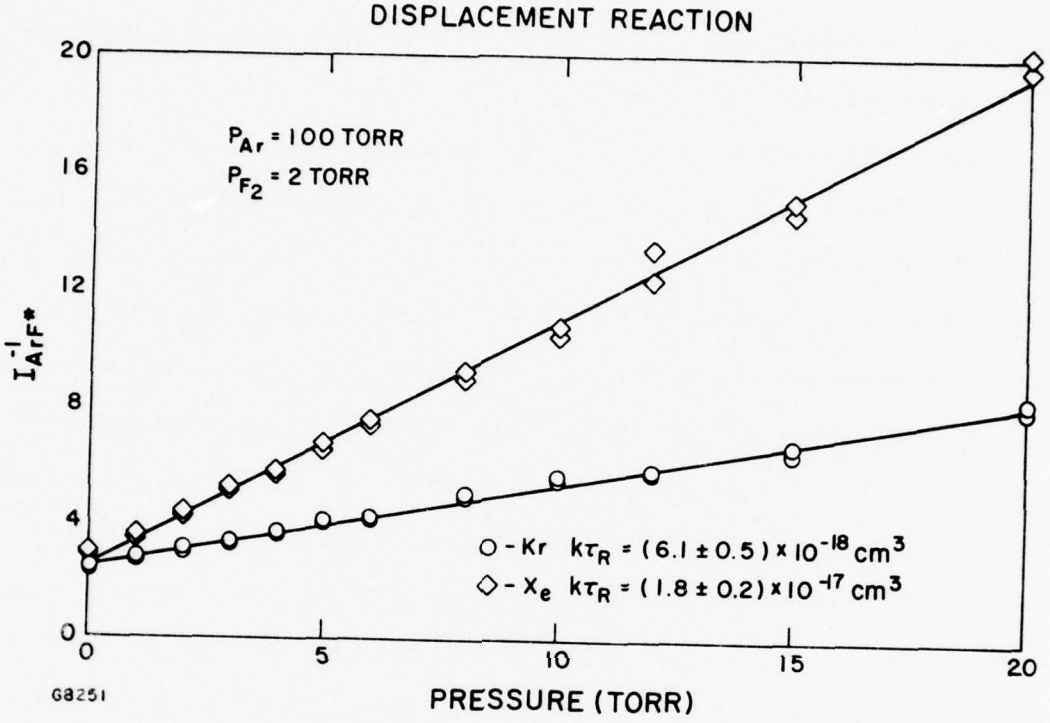

Figure A-4 Stern-Volmer Quenching Curves for ArF* With Xe and Kr

also measured by observing the increase in the KrF* and XeF* fluorescence with increasing Kr and Xe, respectively. These measurements give the same rate constants to within 10%, so we conclude that Kr and Xe displaces ArF* respectively with unit branching ratios.

The radiative lifetime of ArF* has been calculated to be 4 ns by Dunning and Hay.[10] Such a short lifetime gives quenching rate constants of ArF* by Kr and Xe to be 1.6×10^{-9} and 4.5×10^{-9} cm^3/sec, respectively. These rate constants seem unusually large even for this type of reaction. For example, the kinetically similar alkali-halide reaction Rb + KF → RbF + K has a rate constant about an order of magnitude smaller than these rare-gas-halide displacement reactions.[15] One possible reason for the difference is the much higher exothermicity of the rare-gas-halide displacement reactions.[16] Another explanation for the rapid displacement rate constants is that the Kr (or Xe) atom displaces the Ar atom when the ArF* is in a high vibrational level. This would be especially true for the ArF* formed through the ion channel (reaction (3) of Table A-2).

The authors acknowledge many discussions with Dr. C.W. vonRosenberg, Jr.

(15) S. Stofte, A.E. Procter, and R.B. Bernstein, J. Chem. Phys. 65, 4990 (1976).

(16) M. Krauss (private communication).

APPENDIX A

REFERENCES

1. A. Hawryluk, J.A. Mangano, and J.H. Jacob, 3rd Summer Colloquium on Electronic Transition Lasers, 1976 (unpublished).

2. D.C. Lorents, R.M. Hill, D.L. Huestis, M.V. McCusker, and N.H. Nakano, in Ref. 1.

3. J.E. Velazco, J.H. Kolts and D.W. Setser, J. Chem. Phys. 65, 3468 (1976).

4. J.A. Mangano, J.H. Jacob, M. Rokni, and A. Hawryluk, Appl. Phys. Lett. 31, 26 (1977).

5. H.C. Brashears, Jr., D.W. Setser, and D. MesMarteau (unpublished).

6. M. Rokni, J.H. Jacob, J.A. Mangano, and R. Brochu, Appl. Phys. Lett. 30, 458 (1977).

7. D.W. Setser (private communication).

8. J.M. Hoffman, A.K. Hays, and G.C. Tisone, Appl. Phys. Lett. 28, 538 (1976).

9. M. Krauss (private communication).

10. T.H. Dunning and P.J. Hay, 7th Winter Colloquium on High Power Visible Lasers, Park City, Utah, 1977 (unpublished).

11. J.A. Mangano and J.H. Jacob, Appl. Phys. Lett. 27, 495 (1975).

12. It was determined aposterion that at 150 torr the Ar quenching of ArF* introduces a 5% error. This error was corrected for subsequently.

13. About 10% of the e-beam power goes directly into producing the rare-gas metastables. See for example, L.R. Peterson and J.E. Allen, J. Chem. Phys. 56, 6068 (1972). In the experiments performed the primary loss for Ar* is by F_2 quenching to form ArF*.

14. D.K. Bohme, N.G. Adams, M. Moselman, D.B. Dunkin, and E.E. Ferguson, J. Chem. Phys. 52, 5094 (1970).

15. S. Stofte, A.E. Procter, and R.B. Bernstein, J. Chem. Phys. 65, 4990 (1976).

16. M. Krauss (private communication).

APPENDIX B

THREE-BODY QUENCHING OF KrF* BY Ar AND BROAD-BAND EMISSION AT 415 nm

APPENDIX B

THREE-BODY QUENCHING OF KrF* BY Ar AND BROAD-BAND EMISSION AT 415 nm

In this letter measurements of the KrF* ($B^2\Sigma_{1/2} \rightarrow X^2\Sigma_{1/2}$) fluorescence efficiency as a function of mixture ratio and pressure are given for e-beam-excited $Ar/Kr/F_2$ mixtures. Mixtures containing 0.3% F_2 and $\leq$ 15% Kr were studied since they are typical of those used in KrF* lasers. The electron-gun apparatus, capable of delivering a beam with an energy of 150 keV and a current density of 0.16-5 A/cm^2 for 300 nsec, has been described previously.[1] The cross-sectional dimensions of the e-beam were 2 cm x 22 cm. The beam deposited its energy in the gas mixture which was contained in a Teflon cell. The cell was 0.5 cm long in the beam direction to ensure uniform energy deposition over the volume of the cell up to pressures of 4 atm.[2]

The KrF* fluorescence amplitude was measured using a pair of apertures to define the solid angle of the detected radiation from the e-beam-excited mixtures. A calibrated photodiode was used to detect the emission. A 5-nm bandpass filter centered at 250 nm was placed in front of the photodiode. The KrF* fluorescence amplitude in W/cm^3 could then be related to the flux seen at the photodiode by integrating over the distributed fluorescence source excited by the electron beam. Isotropic KrF* fluorescence was assumed in this calculation. This condition was assured by utilizing a small beam current density ($\leq$ 5 A/cm^2) to avoid the effects of amplified spontaneous emission. Because KrF is unbound in the ground state the medium is optically thin.

(1) J. A. Mangano and J. H. Jacob, Appl. Phys. Lett. 27, 495 (1975).
(2) J. H. Jacob, J. Appl. Phys. 45, 467 (1974).

The KrF* steady-state fluorescence intensity for mixtures containing 1% and 15% Kr is shown in Figure B-1 as a function of total mixture pressure. Similar data was also taken with mixes containing 3% and 6% Kr. Although the KrF* fluorescence amplitude peaks at pressures of 1.0-2.5 atm, the KrF* laser output (under comparable experimental conditions) from these mixtures can continue to rise with increasing pressure up to approximately 4 atm.[3] In a laser device, the concentration of KrF* can be reduced by a suitably high laser cavity flux which can compete with and perhaps dominate collisional quenching processes. These results imply that the decrease in KrF* fluorescence amplitude for high pressures is caused by quenching of the KrF* directly and is not a process which interferes with the formation of KrF*. Because the cavity dimension in the direction of the e-beam is only 0.5 cm, the energy deposited in the mixture increases linearly with pressure. As a result, if there is no KrF* quenching, the fluorescence will rise linearly with pressure. At high pressures a two-body quenching process will result in a constants radiation with increasing pressure. The KrF* fluorescence data shown in Figure B-1 indicates that the dominant quenching process at high pressure. The KrF* fluorescence amplitude eventually decreases at high pressures.

In order to obtain further information concerning the KrF* quenching processes, spectra shown in Figure B-2 of the spontaneous emission from e-beam-excited mixtures were obtained at mixture pressures of 0.5, 2, and 4 atm. The uncalibrated spectral intensity scale is approximately logarithmic. At 0.5 atm essentially all of the radiation from the mixture is contained in the KrF* $B^2\Sigma_{1/2} \rightarrow X^2\Sigma_{1/2}$ band at 248 nm. However, two other broad bands,

(3) C.A. Brau and J.J. Ewing (private communication).

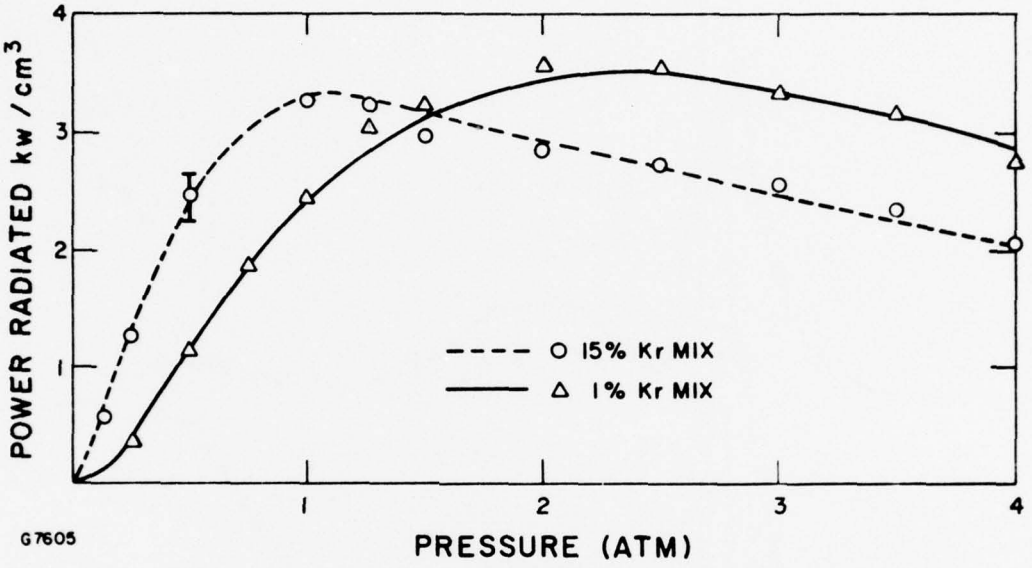

Figure B-1 Curves Showing the Radiated Power on the KrF* $^2\Sigma_{1/2} \rightarrow {}^2\Sigma_{1/2}$ Band as a Function of Total Pressure for 1% and 15% Kr Mixtures. The open triangles and circles are experimental data. The curves are the product of the efficiency given by Eq. (B-4) and the e-beam power deposited.

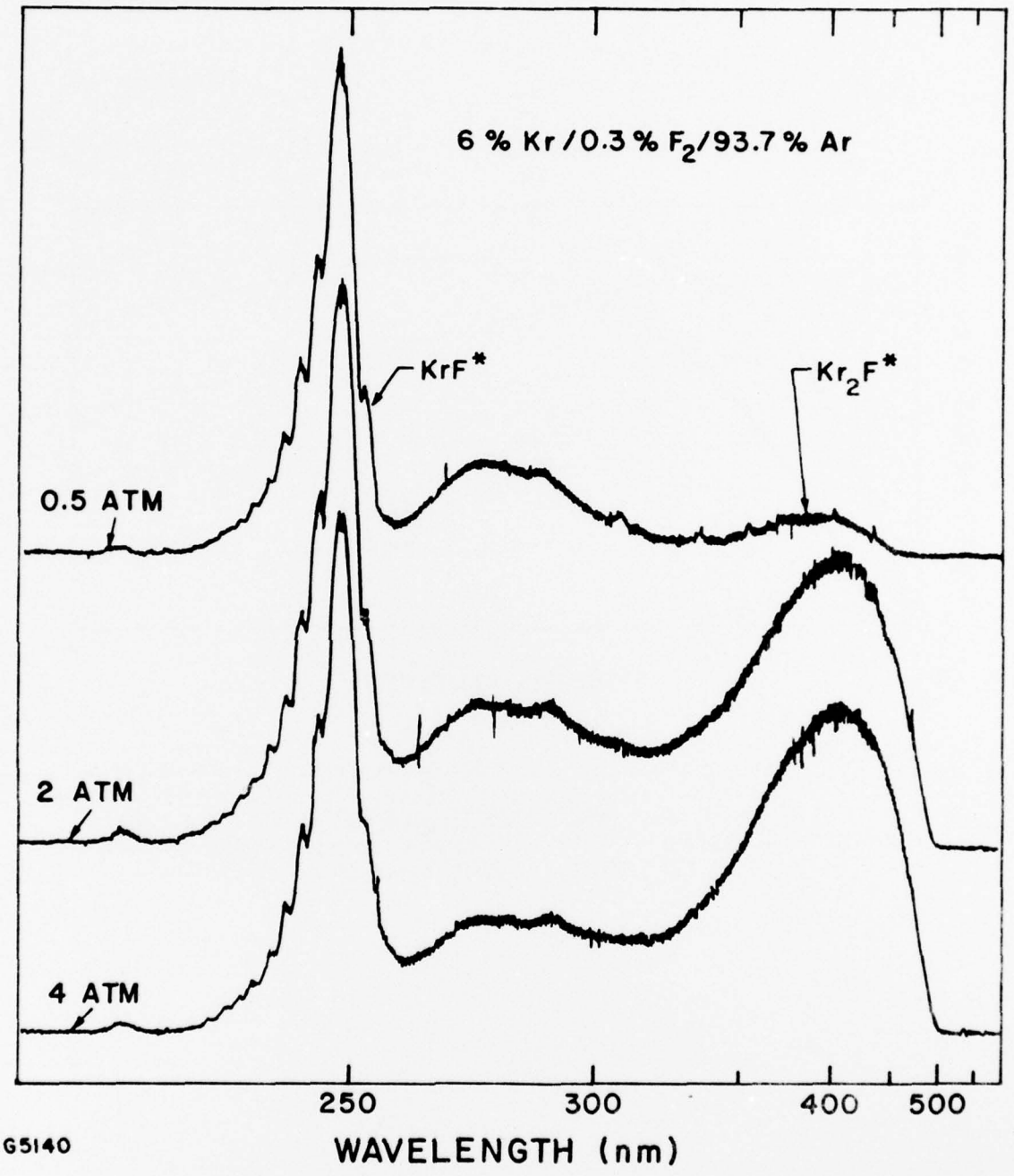

Figure B-2 Spectra from a KrF* Laser Mix at Various Total Pressures

containing much less energy, are observable. The first is centered at 415 nm and has been identified with the $^2B_2 \rightarrow A_1$ transition of the excited triatomic Kr_2F^*.[4] The other broad band, centered roughly at 270-280 nm, is most likely a combination of radiation from the $^2\Sigma - ^2\Pi$ band of KrF* and perhaps radiation from the excited triatomics Ar_2F^*[4] and ArKrF*. Identification of the Kr_2F^* and Ar_2F^* bands was inferred by observing the radiation from binary mixtures of Ar/F_2 and Kr/F_2. From the Kr/F_2 mix we observed the same spectra except that some of the structure in the band centered at 270-280 nm disappeared. From the Ar/F_2 mixture, the spectra showed only a very broad band centered at 290-300 nm which has been identified as Ar_2F^* radiation. The spectrum obtained at a total mixture pressure of 4 atm indicates that, compared with the 0.5-atm spectrum, essentially the same energy is contained in the KrF* $B^2\Sigma_{1/2} \rightarrow X^2\Sigma_{1/2}$ band, although the e-beam energy deposited increased by a factor of ~ 8. This spectrum indicates that most of the additional energy deposited by the e-beam was channeled to Kr_2F^* Consequently (because of the laser result of Ref. 3 and our measurements which will be discussed subsequently), three-body KrF* quenching mechanisms ultimately result in Kr_2F^* formation.

In order to calculate the KrF* fluorescence efficiency from the data shown in Figure B-1, the beam energy density deposited in the mixture was determined by monitoring the pressure rise in the cavity. The steady-state power deposited in the mixture was then calculated. These measurements agreed with beam energy deposition calculations for these mixtures to within 10%.[2] The KrF* fluorescence efficiency (shown in Figure B-3) was then

(4) M. Krauss (private communication).

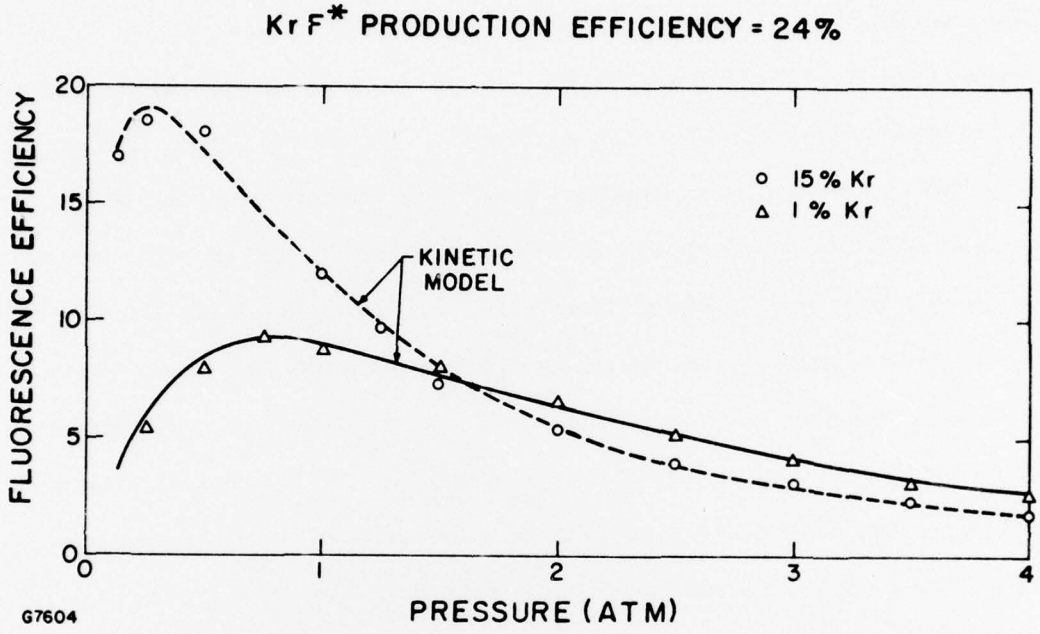

Figure B-3 The Curves are the KrF* Fluorescence Efficiency as Predicted by Eq. (B-4). The points are experimental.

computed as a function of total mixture pressure by dividing the fluorescence amplitudes (shown in Figure B-1) by the corresponding beam power density deposited.

The dominant reactions describing the KrF* formation kinetics at beam current densities of ~ 1 A/cm^2 are listed in Table B-1. Since the mixture contains ≥ 85% argon, the high-energy beam electrons $\vec{e}$ deposit most of their energy into the argon. Approximately 55% of this energy goes into forming argon ions,[5] Ar^+. At low pressures (< 1 atm), these ions rapidly recombine with the negative ions F^- with a diffusion-limited equivalent two-body rate constant of approximately (2-3) x 10^{-6} cm^3/sec[6] to form ArF*. The ArF* can radiate at 193 nm and form ground-state Ar and F atoms (reaction 4). The radiative lifetime of ArF* has been calculated to be 10 nsec.[7] However, at sufficiently high krypton number densities, the krypton will exchange with the ArF* to form KrF* (reaction 5).[8] In fact, the decrease in the KrF* fluorescence efficiency seen in Figure B-3 at low total mixture pressures can be explained if some significant number of the ArF* radiate before the exchange reaction can occur.

At high pressure the argon ions and neutrals form Ar_2^+ with a three-body rate constant of 2.5 x 10^{-31} cm^6/sec.[9] The Ar_2^+ can undergo charge

(5) L.R. Peterson and J.E. Allen, J. Chem. Phys. 56, 6068 (1972).

(6) M.R. Flannery, in Case Studies in Atomic Collision Physics 2, edited by E.W. McDaniel and M.R.C. McDowell (North-Holland, Amsterdam, 1972), p. 3.

(7) H. Michels (private communication).

(8) J.J. Ewing (private communication).

(9) E.W. McDaniel, V. Ermak, A. Dalgarno, E.E. Ferguson, and L. Friedman, Ion-Molecule Reactions (Wiley-Interscience, New York, 1970), p. 338.

TABLE B-1. FORMATION KINETICS

e-beam ionization		
$\vec{e} + Ar \rightarrow Ar^+ + \vec{e} + e_s$		(1)
Low Pressure		
$e_s + F_2 \rightarrow F^- + F$	$2\text{-}3 \times 10^{-9}$ cm^3/sec	(2)
$F^- + Ar^+ + (M) \rightarrow ArF^* + (M)$		(3)
$ArF^* \rightarrow Ar + F + h\nu$	10 nsec	(4)
$ArF^* + Kr \rightarrow KrF^* + Ar$	5×10^{-10} cm^3/sec	(5)
High Pressure		
$Ar^+ + Ar + M \rightarrow Ar_2^+ + M$	2.5×10^{-31} cm^6/sec	(6)
$Ar_2^+ + Kr \rightarrow Kr^+ + 2Ar$	7.5×10^{-10} cm^3/sec	(7)
$Kr^+ + F^- + M \rightarrow KrF^* + M$	$(2\text{-}3) \times 10^{-6}$ cm^3/sec	(8)
$Kr^+ + Kr + M \rightarrow Kr_2^+ + M$	2.5×10^{-31} cm^6/sec	(9)
$Kr_2^+ + F^- \rightarrow KrF^* + Kr$	$(2\text{-}3) \times 10^{-6}$ cm^3/sec	(10)

transfers with Kr to form Kr^+ with a rate constant of 7.5×10^{-10} cm^3/sec.[10] For lean krypton mixes the Kr^+ will combine with the negative fluorine ions to form KrF*. As the Kr density is increased, Kr_2^+ will be formed. By varying the e-beam pump power by a factor of 30, we have verified that Kr_2^+ recombines with F^- to form KrF*.[11] The KrF* can spontaneously decay with a lifetime of 6.5 nsec (calculated by Dunning and Hay)[12] or can be collisionally quenched. Three-body quenching of KrF* is primarily responsible for the decrease in the KrF* fluorescence efficiency seen at higher pressures. From Figure B-3 this collisional quenching is seen to be dependent on the krypton density. The dominant KrF* quenching mechanisms consistent with all the data presented above are two-body quenching by F_2[13]

$$KrF^* + F_2 \xrightarrow{k_1} \text{products}, \tag{B-1}$$

three-body quenching by Ar

$$KrF^* + 2Ar \xrightarrow{k_2} \text{products}, \tag{B-2}$$

and three-body quenching by Kr

$$KrF^* + Kr + Ar \xrightarrow{k_2} \text{products}. \tag{B-3}$$

We postulate that ArKrF* is formed by reaction (2) and is rapidly displaced to form Kr_2F^*. In reaction (3) Kr_2F^* can be formed directly. The excited triatomic Kr_2F^* then radiates ($^2B_2 \rightarrow A_1$) to give a broad band centered at

(10) D.K. Bohme, N.G. Adams, M. Moselman, D.B. Dunkin, and E.E. Ferguson, J. Chem. Phys. 52, 5094 (1970).

(11) For a detailed discussion of this verification procedure see M. Rokni, J.H. Jacob, J.A. Mangano, and R. Brochu, Appl. Phys. Lett. 30, 458 (1977).

(12) T.H. Dunning and P.J. Hay, Appl. Phys. Lett. 28, 649 (1976).

(13) M. Rokni, J.H. Jacob, and J.A. Mangano (unpublished).

415 nm. The products $k_2\tau_1$ of the rate constants (for the KrF* quenching) and the radiative lifetime τ_1 can be determined by fitting the predictions of the kinetic model summarized in Table B-1 and above to the KrF* fluorescence efficiency data. At high pressures (> 1 atm) the resulting fit is especially sensitive to the value assumed for these products. Using the measured value of $k_1\tau_1 = 5 \times 10^{-18}$ cm^3 (Ref. 2) and analyzing all the data we have determined the products $k_2\tau_1$ and $k_3\tau_1$. For mixes containing 1% Kr the effect of reaction (3) on the quenching of KrF* is $\leq 10\%$. So, from the very lean Kr mixes, a value of $k_2\tau_1$ is measured to be

$$k_2\tau_1 = (5.2 \pm 0.5) \times 10^{-40} \text{ cm}^6.$$

As the Kr partial pressure is increased reaction (3) becomes more important and analyzing the data for the various mixes, the $k_3\tau_1$ product is determined to be

$$k_3\tau_1 = (4.2 \pm 1) \times 10^{-39} \text{ cm}^6.$$

Assuming the Dunning and Hay[12] calculated KrF* lifetime of 6.5 nsec, $k_2 = 8 \times 10^{-32}$ cm^6/sec and $k_3 = 6.5 \times 10^{-31}$ cm^6/sec.

At low pressures (< 0.5 atm), the KrF* fluorescence efficiency is sensitive to the product of the rate constant, k_e, for the exchange reaction

$$\text{Kr} + \text{ArF}^* \xrightarrow{k_e} \text{KrF}^* + \text{Ar}$$

and the ArF* radiative lifetime τ_2. The value for this product giving the best fit to the low-pressure data is[13]

$$k_e\tau_2 = (5.5 \pm 0.7) \times 10^{-18} \text{ cm}^3.$$

Assuming the value of the ArF* radiative lifetime calculated by Michels,[7] 10 nsec, the exchange rate constant k_e is 5.5×10^{-10} cm^3/sec.[14] Combination of the exchange reaction and the three-body quenching results in the following approximate expression for the steady-state[15] fluorescence efficiency η:

$$\eta \approx \eta_M \left(\frac{k_e \tau_2 N_{Kr}}{1 + k_e \tau_2 N_{Kr}}\right)\left(\frac{1}{1 + k_1 \tau_1 N_{F_2} + k_2 \tau_1 N_{Ar}^2 + k_3 \tau_1 N_{Kr} N_{Ar}}\right), \quad \text{(B-4)}$$

where N_{Kr} is the density of krypton, N_{F_2} is the density of F_2, and N_{Ar} is the argon density. The code agrees with Eq. (B-4), over the parameter range investigated in this paper, to within 10%. The maximum efficiency η_M for producing KrF* is about 25%. The curves shown in Figure B-3 are a plot of Eq. (B-4). In Figure B-1 the curves plotted are the product of η and the e-beam power deposited.

The saturation flux can now be calculated for the KrF* laser. If the KrF* quenching processes are included, the saturation flux can be written as

$$\phi_{SAT} = (h\nu/\sigma_s \tau_1)(1 + k_1 \tau_1 N_{F_2} + k_2 \tau_1 N_{Ar}^2 + k_3 \tau_1 N_{Kr} N_{Ar}), \quad \text{(B-5)}$$

where $h\nu$ is the KrF* photon energy (5 eV) and σ_s is the stimulated emission cross section. The product of the KrF* stimulated emission cross section and lifetime have been measured to be 1.6×10^{-24} cm^2 sec.[16] This

(14) We have recently measured the exchange reaction by observing the decrease in the ArF* fluorescence and obtained a value of $k_e \approx 6.5 \times 10^{-18}$ cm^3/sec. This work was reported by us at the 7th Winter Colloquium on High Power Visible Lasers, Park City, Utah, 1977.

(15) The steady-state assumption is valid because the dominant inverse rates are much less than the 300-ns e-beam pulse length.

(16) A. Hawryluk, J. A. Mangano, and J. H. Jacob, Proceedings of the Third Summer Colloquium on Electronic Transition Lasers, Snowmass, 1976 (unpublished).

result is in good agreement with that inferred by Tellinghuisen et al[17] by analyzing the KrF* fluorescence spectrum. Using the measured value of $\sigma_s \tau_1$ and Eq. (B-5), the saturation flux for the KrF* laser is approximately 0.85 MW/cm^2 for a mixture containing 0.3% F_2 and 1% Kr at a total pressure of 1 atm.

The authors wish to thank Dr. M. Krauss for suggesting the interpretation of the spectra shown in Figure B-2. Numerous informative discussions with Dr. D. Trainor concerning the kinetic channeling proposed here are also acknowledged.

(17) J. Tellinghuisen, A.K. Hays, J.M. Hoffman, and G.C. Tisone, J. Chem. Phys. 65, 4473 (1975).

APPENDIX B

REFERENCES

1. J. A. Mangano and J. H. Jacob, Appl. Phys. Lett. 27, 495 (1975).

2. J. H. Jacob, J. Appl. Phys. 45, 467 (1974).

3. C. A. Brau and J. J. Ewing (private communication).

4. M. Krauss (private communication).

5. L. R. Peterson and J. E. Allen, J. Chem. Phys. 56, 6068 (1972).

6. M. R. Flannery, in Case Studies in Atomic Collision Physics 2, edited by E. W. McDaniel and M. R. C. McDowell (North-Holland, Amsterdam, 1972), p. 3.

7. H. Michels (private communication).

8. J. J. Ewing (private communication).

9. E. W. McDaniel, V. Ermak, A. Dalgarno, E. E. Ferguson, and L. Friedman, Ion-Molecule Reactions (Wiley-Interscience, New York, 1970), p. 338.

10. D. K. Bohme, N. G. Adams, M. Moselman, D. B. Dunkin, and E. E. Ferguson, J. Chem. Phys. 52, 5094 (1970).

11. For a detailed discussion of this verification procedure see M. Rokni, J. H. Jacob, J. A. Mangano, and R. Brochu, Appl. Phys. Lett. 30, 458 (1977).

12. T. H. Dunning and P. J. Hay, Appl. Phys. Lett. 28, 649 (1976).

13. M. Rokni, J. H. Jacob, and J. A. Mangano (unpublished).

14. We have recently measured the exchange reaction by observing the decrease in the ArF* fluorescence and obtained a value of $k_e \approx 6.5 \times 10^{-18}$ cm^3/sec. This work was reported by us at the 7th Winter Colloquium on High Power Visible Lasers, Park City, Utah, 1977.

15. The steady-state assumption is valid because the dominant inverse rates are much less than the 300-ns e-beam pulse length.

16. A. Hawryluk, J. A. Mangano, and J. H. Jacob, Proceedings of the Third Summer Colloquium on Electronic Transition Lasers, Snowmass, 1976 (unpublished).

17. J. Tellinghuisen, A. K. Hays, J. M. Hoffman, and G. C. Tisone, J. Chem. Phys. 65, 4473 (1975).

DISTRIBUTION LIST

Office of Naval Research, Department of the Navy, Arlington, VA 22217 - Attn: Physics Program (3 copies)

Naval Research Laboratory, Department of the Navy, Washington, D.C. 20375 - Attn: Technical Library (1 copy)

Office of the Director of Defense, Research and Engineering, *Information Office Library Branch, The Pentagon, Washington,* D.C. 20301 (1 copy)

U.S. Army Research Office, Box CM, Duke Station, Durham, N.C. 27706 (1 copy)

Defense Documentation Center, Cameron Station, Alexandria, VA 22314 (12 copies)

Defender Information Analysis Center, Battelle Memorial Institute, 505 King Avenue, Columbus, OH 43201 (1 copy)

Commanding Officer, Office of Naval Research Branch Office, 536 South Clark Street, Chicago, IL 60615 (1 copy)

New York Area Office, Office of Naval Research, 715 Broadway (5th Floor), New York, NY 10003 - Attn: Dr. Irving Rowe (1 copy)

San Francisco Area Office, Office of Naval Research, 760 Market Street, Room 447, San Francisco, CA 94102 (1 copy)

Air Force Office of Scientific Research, *Department of the Air Force, Washington,* D.C. 22209 (1 copy)

Office of Naval Research Branch Office, 1030 East Green Street, Pasadena, CA 91106 - Attn: Dr. Robert Behringer (1 copy)

Code 102 1P (ONRL), Office of Naval Research, 800 N. Quincy Street, Arlington, VA 22217 (6 copies)

Defense Advanced Research Projects Agency, 1400 Wilson Blvd., Arlington, VA 22209 - Attn: Strategic Technology Office (1 copy)

Office Director of Defense, Research & Engineering, The Pentagon, Washington, D.C. 20301 - Attn: Assistant Director (Space and Advanced Systems) (1 copy)

Office of the Assistant Secretary of Defense, System Analysis (Strategic Programs), Washington, D.C. 20301 - Attn: Mr. Gerald R. McNichols (1 copy)

U.S. Arms Control and Disarmament Agency, Dept. of State Bldg., Rm. 4931, Washington, D.C. 20451 - Attn: Dr. Charles Henkin (1 copy)

Energy Research Development Agency, *Division of Military Applications,* Washington, D.C. 20545 (1 copy)

National Aeronautics and Space Administration, Lewis Research Center, Cleveland, OH 44135 - Attn: Dr. John W. Dunning, Jr. (1 copy)
(Aerospace Res. Engineer)

National Aeronautics & Space Administration, Code RR, FOB 10B, 600 Independence Ave., SW, Washington, D.C. 20546 (1 copy)

National Aeronautics and Space Administration, Ames Research Center, Moffett Field, CA 94035 - Attn: Dr. Kenneth W. Billman (1 copy)

Department of the Army, Office of the Chief of RD&A, Washington, D.C. 20310 - Attn: DARD-DD (1 copy)
DAMA-WSM-T (1 copy)

Department of the Army, Office of the Deputy Chief of Staff for Operations & Plans, Washington, D.C. 20310 - Attn: DAMO-RQD - (1 copy)

Ballistic Missile Defense Program Office (BMDPO), The Commonwealth Building, 1300 Wilson Blvd., Arlington, VA 22209 - Attn: Mr. Albert J. Bast, Jr. (1 copy)

U.S. Army Missile Command, Research & Development Division, Redstone Arsenal, AL 35809 - Attn: Army High Energy Laser Programs (2 copies)

Commander, Rock Island Arsenal, Rock Island, IL 61201, Attn: SARRI-LR, Mr. J.W. McGarvey (1 copy)

Commanding Officer, U.S. Army Mobility Equipment R&D Center, Ft. Belvoir, VA 22060 - Attn: SMEFB-MW (1 copy)

Commander, U.S. Army Armament Command, Rock Island, IL 61201 - Attn: AMSAR-RDT (1 copy)

Director, Ballistic Missile Defense Advanced Technology Center, P.O. Box 1500, Huntsville AL 35807 - Attn: ATC-O (1 copy)
ACT-T (1 copy)

Commander, U.S. Army Material Command, Alexandria, VA 22304 - Attn: Mr. Paul Chernoff (AMCRD-T) (1 copy)

Commanding General, U.S. Army Munitions Command, Dover, NH 17801 - Attn: Mr. Gilbert F. Chesnov (AMSMU-R) (1 copy)

Director, U.S. Army Ballistics Res. Lab, Aberdeen Proving Ground, MD 21005 - Attn: Dr. Robert Eichenberger (1 copy)

Commandant, U.S. Army, Air Defense School, Ft. Bliss, TX 79916 - Attn: Air Defense Agency (1 copy)
ATSA-CTD-MS (1 copy)

Commanding General, U.S. Army Combat Dev. Command, Ft. Belvoir, VA 22060 - Attn: Director of Material, Missile Div. (1 copy)

Commander, U.S. Army Training & Doctrine Command, Ft. Monroe, VA 23651 - Attn: ATCD-CF (1 copy)

Commander, U.S. Army Frankford Arsenal, Philadelphia, PA 19137 - Attn: Mr. M. Elnick SARFA-FCD Bldg. 201-3 (1 copy)

Commander, U.S. Army Electronics Command, Ft. Monmouth, NJ 07703 - Attn: AMSEL-CT-L, Dr. R.G. Buser (1 copy)

Commander, U.S. Army Combined Arms Combat Developments Activity, Ft. Leavenworth, KS 66027 (1 copy)

National Security Agency, Ft. Geo. G. Meade, MD 20755 - Attn: R.C. Foss A763 (1 copy)

Deputy Commandant for Combat & Training Developments, U.S. Army Ordnance Center and School, Aberdeen Proving Ground, MD 21005
Attn: ATSL-CTD-MS-R (1 copy)

Commanding Officer, USACDC CBR Agency, Ft. McClellan, AL 36201 - Attn: CDCCBR-MR (Mr. F.D. Poer) (1 copy)

DISTRIBUTION LIST (Continued)

Department of the Navy, Office of the Chief of Naval Operations, The Pentagon 5C739, Washington, D.C. 20350 - Attn: (OP 982F3) (1 copy)

Office of Naval Research Branch Office, 495 Summer Street, Boston, MA 02210 - Attn: Dr. Fred Quelle (1 copy)

Department of the Navy, Deputy Chief of Navy Material (Dev.), Washington, D.C. 20360 - Attn: Mr. R. Gaylord (MAT 032B) (1 copy)

Naval Missile Center, Point Mugu, CA 93042 - Attn: Gary Gibbs (Code 5352) (1 copy)

Naval Research Laboratory, Washington, D.C. 20375 - Attn: (Code 5503-EOTPO) (1 copy)
Dr. P. Livingston - Code 5560 (1 copy)
Dr. A. I. Schindler - Code 6000 (1 copy)
Dr. H. Shenker - Code 5504 (1 copy)
Mr. D.J. McLaughlin - Code 5560 (1 copy)
Dr. John L. Walsh - Code 5503 (1 copy)

High Energy Laser Project Office, Department of the Navy, Naval Sea Systems Command, Washington, D.C. 20360 - Attn: Capt. A. Skolnick, USN (PM 22) (1 copy)

Superintendent, Naval Postgraduate School, Monterey, CA 93940 - Attn: Library (Code 2124) (1 copy)

Navy Radiation Technology, Air Force Weapons Lab (NLO), Kirtland AFB, NM 87117 (1 copy)

Naval Surface Weapons Center, White Oak, Silver Spring, MD 20910 - Attn: Dr. Leon H. Schindel (Code 310) (1 copy)
Dr. E. Leroy Harris (Code 313) (1 copy)
Mr. K. Enkenhaus (Code 034) (1 copy)
Mr. J. Wise (Code 047) (1 copy)
Technical Library (1 copy)

U.S. Naval Weapons Center, China Lake, CA 93555 - Atn: Technical Library (1 copy)

HQ USAF (AF/RDPS), The Pentagon, Washington, D.C. 20330 - Attn: Lt. Col. A.J. Chiota (1 copy)

HQ AFSC/XRLW, Andrews AFB, Washington, D.C. 20331 - Attn: Maj. J.M. Walton (1 copy)

HQ AFSC (DLCAW), Andrews AFB, Washington, D.C. 20331 - Attn: Maj. H. Axelrod (1 copy)

Air Force Weapons Laboratory, Kirtland AFB, NM 87117 - Attn: LR (1 copy)
AL (1 copy)

HQ SAMSO (XRTD), P.O. Box 92960, Worldway Postal Center, Los Angeles, CA 90009 - Attn: Lt. Dorian DeMaio (XRTD) (1 copy)

AF Avionics Lab (TEO), Wright Patterson AFB, OH 45433 - Attn: Mr. K. Hutchinson (1 copy)

Dept. of the Air Force, Air Force Materials Lab. (AFSC), Wright Patterson AFB, OH 45433 - Attn: Maj. Paul Elder (LPS) (1 copy)
Laser Window Group

HQ Aeronautical Systems Div., Wright Patterson AFB, OH 45433 - Attn: XRF - Mr. Clifford Fawcett (1 copy)

Rome Air Development Command, Griffiss AFB, Rome, NY 13440 - Attn: Mr. R. Urtz (OCSE) (1 copy)

HQ Electronics Systems Div. (ESL), L.G. Hanscom Field, Bedford, MA 01730 - Attn: Mr. Alfred E. Anderson (XRT) (1 copy)
Technical Library (1 copy)

Air Force Rocket Propulsion Lab., Edwards AFB, CA 93523 - Attn: B.R. Bornhorst, (LKCG) (1 copy)

Air Force Aero Propulsion Lab., Wright Patterson AFB, OH 45433 - Attn: Col. Walter Moe (CC) (1 copy)

Dept. of the Air Force, Foreign Technology Division, Wright Patterson AFB, OH 45433 - Attn: PDTN (1 copy)

Commandant of the Marine Corps, Scientific Advisor (Code RD-1), Washington, D.C. 20380 (1 copy)

Aerospace Research Labs., (AP), Wright Patterson AFB, OH 45433 - Attn: Lt. Col. Max Duggins (1 copy)

Defense Intelligence Agency, Washington, D.C. 20301 - Attn: Mr. Seymour Berler (DTIB) (1 copy)

Central Intelligence Agency, Washington, D.C. 20505 - Attn: Mr. Julian C. Nall (1 copy)

Analytic Services, Inc., 5613 Leesburg Pike, Falls Church, VA 22041 - Attn: Dr. John Davis (1 copy)

Aerospace Corp., P.O. Box 92957, Los Angeles, CA 90009 - Attn: Dr. G.P. Millburn (1 copy)

Airesearch Manuf. Co., 9851-9951 Sepulveda Blvd., Los Angeles, CA 90009 - Attn: Mr. A. Colin Stancliffe (1 copy)

Atlantic Research Corp., Shirley Highway at Edsall Road, Alexandria, VA 22314 - Attn: Mr. Robert Naismith (1 copy)

Avco Everett Research Lab., 2385 Revere Beach Parkway, Everett, MA 02149 - Attn: Dr. George Sutton (1 copy)
Dr. Jack Daugherty (1 copy)

Battelle Columbus Laboratories, 505 King Avenue, Columbus, OH 43201 - Attn: Mr. Fred Tietzel (STPIAC) (1 copy)

Bell Aerospace Co., Buffalo, NY 14240 - Attn: Dr. Wayne C. Solomon (1 copy)

Boeing Company, P.O. Box 3999, Seattle, WA 98124 - Attn: Mr. M.I. Gamble (2-, 460, MS 8C-88) (1 copy)

Electro-Optical Systems, 300 N. Halstead, Pasadena, CA 91107 - Attn: Dr. Andrew Jensen (1 copy)

ESL, Inc., 495 Java Drive, Sunnyvale, CA 94086 - Attn: Arthur Einhorn (1 copy)

DISTRIBUTION LIST (Continued)

General Electric Co., Space Division, P.O. Box 8555, Philadelphia, PA 19101 - Attn: Dr. R.R. Sigismonti (1 copy)

General Electric Co., 100 Plastics Avenue, Pittsfield, MA 01201 - Attn: Mr. D.G. Harrington (Rm. 1044) (1 copy)

General Research Corp., P.O. Box 3587, Santa Barbara, CA 93105 - Attn: Dr. R. Holbrook (1 copy)

General Research Corp., 1501 Wilson Blvd., Suite 700, Arlington, VA 22209 - Attn: Dr. Giles F. Crimi (1 copy)

Hercules, Inc., Industrial System Dept., Wilmington, DE 19899 - Attn: Dr. R.S. Voris (1 copy)

Hercules, Inc., P.O. Box 210, Cumberland, MD 21502 - Attn: Dr. Ralph R. Preckel (1 copy)

Hughes Research Labs., 3011 Malibu Canyon Road, Malibu, CA 90265 - Attn: Dr. D. Forster (1 copy)

Hughes Aircraft Co., Aerospace Group - Systems Division, Canoga Park, CA 91304 - Attn: Dr. Jack A. Alcalay (1 copy)

Hughes Aircraft Co., Centinela and Teale Streets, Bldg. 6, MS E-125, Culver City, CA 90230 - Attn: Dr. William Yates (1 copy)

Institute for Defense Analyses, 400 Army-Navy Drive, Arlington, VA 22202 - Attn: Dr. Alvin Schnitzler (1 copy)

Johns Hopkins University, Applied Physics Lab., 8621 Georgia Avenue, Silver Spring, MD 20910 - Attn: Dr. Albert M. Stone (1 copy)

Lawrence Livermore Laboratory, P.O. Box 808, Livermore, CA 94550 - Attn: Dr. R.E. Kidder (1 copy)
Dr. E. Teller (1 copy)
Dr. Joe Fleck (1 copy)

Los Alamos Scientific Laboratory, P.O. Box 1663, Los Alamos, NM 87544 - Attn: Dr. Keith Boyer (1 copy)

Lulejian and Associates, Inc., Del Amo Financial Center, 21515 Hawthorne Blvd. - Suite 500, Torrance, CA 90503 (1 copy)

Lockheed Palo Alto Res. Lab., 3251 Hanover St., Palo Alto, CA 94303 - Attn: L.R. Lunsford, Orgn. 52-24, Bldg. 201 (1 copy)

Mathematical Sciences Northwest, Inc., P.O. Box 1887, Bellevue, WN 98009 - Attn: Dr. Abraham Hertzberg (1 copy)

Martin Marietta Corp., P.O. Box 179, Mail Station 0471, Denver, CO 80201 - Attn: Mr. Stewart Chapin (1 copy)

Massachusetts Institute of Technology, Lincoln Laboratory, P.O. Box 73, Lexington, MA 02173 - Attn: Dr. S. Edelberg (1 copy)
Dr. L.C. Marquet (1 copy)

McDonnell Douglas Astronautics Co., 5301 Bolsa Avenue, Huntington Beach, CA 92647 - Attn: Mr. P.L. Klevatt, Dept. A3-830-BBFO, M/S 9 (1 copy)

McDonnell Douglas Research Labs., Dept. 220, Box 516, St. Louis, MO 63166 - Attn: Dr. D.P. Ames (1 copy)

MITRE Corp., P.O. Box 208, Bedford, MA 01730 - Attn: Mr. A.C. Cron (1 copy)

North American Rockwell Corp., Autonetics Div., Anaheim, CA 92803 - Attn: Mr. T.T. Kumagi, C/476 Mail Code HA18 (1 copy)

Northrop Corp., 3401 West Broadway, Hawthorne, CA 90250 - Attn: Dr. Gerard Hasserjian, Laser Systems Dept. (1 copy)

Dr. Anthony N. Pirri, Physical Sciences, Inc., 18 Lakeside Office Park, Wakefield, MA 01880 (1 copy)

RAND Corp., 1700 Main Street, Santa Monica, CA 90406 - Attn: Dr. C.R. Culp/Mr. G.A. Carter (1 copy)

Raytheon Co., 28 Seyon Street, Waltham, MA 02154 - Attn: Dr. F.A. Horrigan (Res. Div.) (1 copy)

Raytheon Co., Boston Post Road, Sudbury, MA 01776 - Attn: Dr. C. Sonnenschien (Equip. Div.) (1 copy)

Raytheon Co., Bedford Labs, Missile Systems Div., Bedford, MA 01730 - Attn: Dr. H.A. Mehlhorn (1 copy)

Riverside Research Institute, 80 West End Street, New York, NY 10023 - Attn: Dr. L.H. O'Neill (1 copy)
Dr. John Bose (1 copy)
(HPEGL Library) (1 copy)

R&D Associates, Inc., P.O. Box 3580, Santa Monica, CA 90431 - Attn: Dr. R.E. LeLevier (1 copy)

Rockwell International Corporation, Rocketdyne Division, Albuquerque District Office, 3636 Menaul Blvd., NE, Suite 211, Albuquerque, NM 87110 - Attn: C.K. Kraus, Mgr. (1 copy)

SANDIA Corp., P.O. Box 5800, Albuquerque, NM 87115 - Attn: Dr. Al Narath (1 copy)

Stanford Research Institute, Menlo Park, CA 94025 - Attn: Dr. F.T. Smith (1 copy)

Science Applications, Inc., 1911 N. Ft. Meyer Drive, Arlington, VA 22209 - Attn: L. Peckam (1 copy)

Science Applications, Inc., P.O. Box 328, Ann Arbor, MI 48103 - Attn: R.E. Meredith (1 copy)

Science Applications, Inc., 6 Preston Court, Bedford, MA 01703 - Attn: R. Greenberg (1 copy)

Science Applications, Inc., P.O. Box 2351, La Jolla, CA 92037 - Attn: Dr. John Asmus (1 copy)

Systems, Science and Software, P.O. Box 1620, La Jolla, CA 92037 - Attn: Alan F. Klein (1 copy)

Systems Consultants, Inc., 1050 31st Street, NW, Washington, D.C. 20007 - Attn: Dr. R.B. Keller (1 copy)

Thiokol Chemical Corp., WASATCH Division, P.O. Box 524, Brigham City, UT 84302 - Attn: Mr. J.E. Hansen (1 copy)

TRW Systems Group, One Space Park, Bldg. R-1, Rm. 1050, Redondo Beach, CA 90278 - Attn: Mr. Norman Campbell (1 copy)

United Technologies Research Center, 400 Main Street, East Hartford, CT 06108 - Attn: Mr. G.H. McLafferty (3 copies)

DISTRIBUTION LIST (Continued)

United Technologies Research Center, Pratt and Whitney Aircraft Div., Florida R&D Center, West Palm Beach, FL 33402 Attn: Dr. R.A. Schmidtke (1 copy)
Mr. Ed Pinsley (1 copy)

VARIAN Associates, EIMAC Division, 301 Industrial Way, San Carlos, CA 94070 - Attn: Mr. Jack Quinn (1 copy)

Vought Systems Division, LTV Aerospace Corp., P.O. Box 5907, Dallas, TX 75222 - Attn: Mr. F.G. Simpson, MS 254142 (1 copy)

Westinghouse Electric Corp., Defense and Space Center, Balt-Wash. International Airport - Box 746, Baltimore, MD 21203 - Attn: Mr. W.F. List (1 copy)

Westinghouse Research Labs., Beulah Road, Churchill Boro, Pittsburgh, PA 15235 - Attn: Dr. E.P. Riedel (1 copy)

United Technologies Research Center, East Hartford, CT 06108 - Attn: A.J. DeMaria (1 copy)

Airborne Instruments Laboratory, Walt Whitorian Road, Melville, NY 11746 - Attn: F. Pace (1 copy)

General Electric R&D Center, Schenectady, NY 12305 - Attn: Dr. Donald White (1 copy)

Cleveland State University, Cleveland, OH 44115 - Attn: Dean Jack Soules (1 copy)

EXXON Research and Engineering Co., P.O. Box 8, Linden, NJ 07036 - Attn: D. Grafstein (1 copy)

University of Maryland, Department of Physics and Astronomy, College Park, MD 20742 - Attn: D. Currie (1 copy)

Sylvania Electric Products, Inc., 100 Fergeson Drive, Mountain View, CA 94040 - Attn: L.M. Osterink (1 copy)

North American Rockwell Corp., Autonetics Division, 3370 Miraloma Avenue, Anaheim, CA 92803 - Attn: R. Gudmundsen (1 copy)

Massachusetts Institute of Technology, 77 Massachusetts Avenue, Cambridge, MA 02138 - Attn: Prof. A. Javan (1 copy)

Lockheed Missile & Space Co., Palo Alto Research Laboratories, Palo Alto, CA 94304 - Attn: Dr. R.C. Ohlman (1 copy)

ILC Laboratories, Inc., 164 Commercial Street, Sunnyvale, GA 94086 - Attn: L. Noble (1 copy)

University of Texas at Dallas, P.O. Box 30365, Dallas, TX 75230 - Attn: Prof. Carl B. Collins (1 copy)

Polytechnic Institute of New York, Rt. 110, Farmingdale, NY 11735 - Attn: Dr. William T. Walter (1 copy)